Macrophages utilize a bet-hedging strategy for antimicrobial activity in phagolysosomal acidification

Quigly Dragotakes[1], Kaitlin Stouffer[1], Man Shun Fu[1], Yehonatan Sella[3], Christine Youn[2], Insun Yoon[4], Carlos M. De Leon-Rodriguez[1], Joudeh B. Freij[1], Aviv Bergman[3,5,¥] and Arturo Casadevall[1,¥,*]

[1]Department of Molecular Microbiology and Immunology, Johns Hopkins School of Public Health, Baltimore, MD, [2]Department of Cellular and Molecular Medicine, Johns Hopkins School of Medicine, Baltimore, MD, [3]Department of Systems and Computational Biology, Albert Einstein College of Medicine, Bronx, NY, [4]Johns Hopkins University, and [5]Santa Fe Institute, Santa Fe, NM.

[¥]A.B. and A.C. share senior authorship

Running title: Chance contributes to host defense

Declaration of Interests

The authors declare no competing interests.

*Address correspondence:

Arturo Casadevall MD, PhD
Johns Hopkins School of Public Health
615 N. Wolfe Street
Room E5132
Baltimore, Maryland 21205

Abstract

Microbial ingestion by a macrophage results in the formation of an acidic phagolysosome but the host cell has no information on the pH susceptibility of the ingested organism. This poses a problem for the macrophage and raises the fundamental question of how the phagocytic cell optimizes the acidification process to prevail. We analyzed the dynamical distribution of phagolysosomal pH in murine and human macrophages that had ingested live or dead *Cryptococcus neoformans* cells, or inert beads. Phagolysosomal acidification produced a range of pH values that approximated normal distributions, but these differed from normality depending on ingested particle type. Analysis of the increments of pH reduction revealed no forbidden ordinal patterns, implying that phagosomal acidification process was a stochastic dynamical system. Using simulation modeling, we determined that by stochastically acidifying a phagolysosome to a pH within the observed distribution, macrophages sacrificed a small amount of overall fitness to reduce their overall variation in fitness. Hence, chance in the final phagosomal pH introduces unpredictability to the outcome of the macrophage-microbe, which implies a bet-hedging strategy that benefits the macrophage. While bet hedging is common in biological systems at the organism level, our results show its use at the organelle and cellular level.

Keywords (up to 10): Cryptococcus neoformans, Chaos, Bet-hedging, phagolysosome, trained immunity, chance, fungal, disease

Introduction

***Audaces fortuna iuvat* (Fortune favors the bold) - Virgil**

Phagocytosis is a fundamental cellular process used by unicellular organisms for nutrient acquisition as well as by host immune cells for microbial defense. The parallels between food acquisition and immunity have led to the suggestion that these two processes had a common evolutionary origin(1). The process of phagocytosis results in the formation of a phagolysosome, a dynamic membrane bounded organelle, which represents a critical location in the struggle between the host and ingested microbial cells(2). Microbial ingestion into phagosomes results in exposure to host cell microbicidal mechanisms, which leads to death for some microbes while others survive by subverting critical aspects of phagosome maturation and by damaging phagolysosome structural integrity.

The process of phagosomal maturation, encompassed by the fusion of the phagosome with lysosomes and lumen acidification, is a complex choreography that includes the recruitment of V-ATPase from lysosomes to the phagolysosome(2, 3) and many other protein components(4). Proton pumping into phagolysosomal lumen results in acidification that inhibits microbes and activates antimicrobial processes that are microbicidal. Consequently, some types of microbes, such as *Mycobacterium tuberculosis* and *Histoplasma capsulatum*, interfere with phagosomal maturation and acidification to promote their intracellular survival. The extent of phagosomal acidification is determined by numerous mechanisms that include proton flux through the pump, proton consumption in the phagosomal lumen, and backflow into the cytoplasm(5). Phagosome acidification in macrophages is rapid with a pH of 6 being reached within 10 min after ingestion(6) and 5.4 by 15-20 min(7).

Cryptococcus neoformans is a facultative intracellular pathogen(8). Upon ingestion by macrophages, *C. neoformans* resides in a mature acidic phagolysosome(9). The outcome of macrophage-*C. neoformans* interaction is highly variable depending on whether the fungal cell is killed, inhibited, or unaltered. If not killed, *C. neoformans* can replicate intracellularly, resulting in variable outcomes which include death and lysis of the host cell, non-lytic exocytosis(10, 11), transfer to another macrophage(12, 13), or phagosomal persistence. A critical variable in determining the outcome of the *C. neoformans*-macrophage interaction is phagosomal membrane integrity, with maintenance of this barrier conducive to control of intracellular infection while loss of integrity leads to host cell death(14).

Prior studies of *C. neoformans* phagosomal acidification measured great variation in the pH of individual phagolysosomes(14–16). The pH of cryptococcal phagolysosomes is affected by several microbial variables that include urease expression(15), phagosomal membrane integrity(14), and the presence of the cryptococcal capsule with glucuronic acid residues that can influence the final pH via acid base properties(17). In addition, the capsule of *C. neoformans* increases in diameter as part of a stress response

which can potentially affect the phagolysosomal pH through increasing the phagolysosome volume, thus diluting its contents and promoting membrane damage through physical stress(14).

In this study, we analyzed the time dependence of the phagolysosomal pH distribution in murine and human macrophages and conclude that acidification is a stochastic process in which macrophages default to a range of pHs with random variation. We demonstrate that, in doing so, macrophages employ a bet-hedging strategy by sacrificing a small amount of overall fitness to ensure broad survivability. Thus, we suggest that chance, in the form of stochastic dynamics, could be an important strategy in phagosomal acidification, which benefits the macrophage by bet hedging against a range of pathogens, and could echo through the immune process to introduce a fundamental uncertainty in the outcome of microbe-macrophage interactions.

Results

We previously reported a wide distribution of phagolysosomal pH after the ingestion of *C. neoformans* by murine bone marrow derived macrophages (BMDMs) (14, 15). Given that the growth rate of *C. neoformans* is highly affected by pH(15, 18) and that the outcome of the *C. neoformans*-macrophage interaction is determined in the phagolysosome(14, 19, 20), we analyzed the distribution of phagolysosomal pH mathematically to gain insight into the dynamics of the acidification process. A scheme of the method used to determine phagosomal acidification with representative data from polystyrene bead phagocytosis experiments are shown in Supplemental Figure 1.

Murine macrophage phagolysosomes acidify stochastically

To determine whether phagolysosomal acidification is a deterministic or stochastic dynamical process, we employed a permutation spectrum test(21) in which the distribution of ordinal patterns occurring in subsets of our full dataset was analyzed (SFig 1C). We found no forbidden patterns at any time evaluated for any of the pH distributions resulting from the ingestion of beads, alive *C. neoformans,* or heat-killed *C. neoformans*, which implies that the acidification is a stochastic process (Figure 1). This analysis was repeated on several other strains and conditions throughout the project and at no point did we observe forbidden ordinal patterns (SFig 2A). Given that beads are inert and cannot modify pH, we reasoned that their corresponding phagolysosomes would be the closest approximation of a default acidification state and would therefore represent a “baseline” to which we could compare phagolysosome acidification dynamics in other conditions.

Bead ingested murine macrophage phagolysosomes stabilize to a normally distributed pH

To probe the dynamics of the phagolysosomal acidification system at this baseline, we analyzed several hundred individual phagolysosomal pH measurements at various time intervals after BMDMs had

114 ingested inert beads (Figure 2A). To determine whether phagolysosome pH measurements followed a
115 normal distribution, the measured relative pH values were fit to a predicted normal distribution using the
116 "fitdistrplus" R statistical package then analyzed via Q-Q plots and the Shapiro-Wilk normality test. We
117 found that phagolysosome pH value distributions did not approximate normality at early times (15 and 30
118 min), but mostly did at intervals of and past 1 h post infection. We were able to reject the Shapiro-Wilk
119 null hypothesis only at 15 min, 30 min, and 3 h (Figure 2B). We hypothesized that not all phagolysosomes
120 were fully mature before 1 h and reasoned that the bimodal appearance of pH at early time intervals is
121 likely due to the population of phagosomes being at different stages of maturity. Interestingly, the pH
122 distribution for the phagolysosomes containing live or dead *C. neoformans* did not approximate normality
123 even at later times. We rejected Shapiro-Wilk normality for each of these samples except for dead *C.*
124 *neoformans* at 3 h. Q-Q plots supported the notion that each sample skews further from normality
125 compared to bead ingested macrophage phagolysosome pH distributions (SFig 3). Considering that
126 macrophages default to a random pH from a particular normal distribution and that *C. neoformans* invest
127 in disrupting this process, we hypothesized that this system must confer some host benefit. Thus, we
128 decided to compare the pH distribution of mature bead ingested phagolysosomes to a range of pHs
129 tolerated by relevant potential pathogens.

130

131 <u>BMDM phagolysosomes acidify to a pH range suboptimal for growth of soil and pathogenic microbes</u>

132 The pH of soils varies greatly from acidic to alkaline based on a variety of conditions that, in turn,
133 determine the associated microbiome(22). Soils contain many pathogenic microbes including *C.*
134 *neoformans*. Since the phagolysosome is an acidic environment, we reasoned that microbes that thrive in
135 acidic soils could proxy for the types of microbes that hosts, and thus macrophages, could encounter, and
136 pose a threat to the cell/host due to their acidophilic nature (ex. *Cryptococcus neoformans*). Hence, we
137 compared(23, 24) the distribution of pH values from mature phagolysosomes (HPI ≥ 1 h) which had
138 ingested latex beads, as a measure of the range of acidities generated in the absence of microbial
139 modulation, relative to published soil microbe growth data as a function of pH (Figure 3). The latex bead
140 pH distribution is narrow and centered at a pH of about 4.5, which corresponds to a pH that significantly
141 reduces the optimal growth even for microbes in acidic soils. To generate a more relevant comparison to
142 human disease models, we also searched out the pH tolerance of 27 significant human pathogens which
143 macrophages are likely to encounter during human infectious diseases (Supplemental Table I). We then
144 compared these distributions to the pH distribution in bead ingested macrophage phagolysosomes (Figure
145 3). The distribution of this default macrophage pH heavily overlaps with the more inhibitory pH regions
146 when compared to both soil and known pathogen pH tolerances. Taken together these data suggest that
147 the low phagosomal pH is itself a defense mechanism, with a distribution that manifests bet hedging by
148 defaulting to a range, rather than single value, inhibitory to most of the spectrum of pathogens the
149 macrophage is likely to encounter.

150

151 <u>Simulations of macrophage populations show stochastic pH as a bet-hedging strategy</u>

152 Bet-hedging is generally understood as a strategy which decreases the variation in fitness at the expense
153 of a small decrease in mean fitness. To test whether variation in macrophage phagolysosome pH
154 constitutes a diversified bet-hedging strategy, we first modeled host survival rate as a function of final
155 phagolysosomal pH in the context of a pathogen randomly selected from Supplemental Table I. This
156 analysis modeled phagolysosomal pH as a normal distribution with mean μ and standard deviation σ
157 varied over a range of possible values in order to test how bet-hedging depends on these parameters. To
158 each phagolysosomal pH, we associated a fitness value which models survival likelihood against
159 pathogens, using the list of pathogens (Table 1), with their viable pH ranges collected from the literature,
160 and we computed the distribution of fitness (p) as phagolysosomal pH varies (Figure 4A,B). As expected
161 in bet-hedging, we observed concurrent decreases in mean fitness and standard deviation of fitness with
162 increasing σ of phagolysosomal pH.

163 Another way to formalize the emergence of bet-hedging as an evolutionary strategy is by considering the
164 average long-term rate of growth. Thus, we considered a multiplicative model, in which the growth rate
165 (r_T) over time (T) was defined as the geometric mean of ρ_t, where ρ_t is the fitness at time t and t ranges
166 from 1 to T. Taking logs, log(r_T) is the average of the random variable log(ρ_t). By the law of large numbers,
167 this average will approach E(log(ρ_t)). Thus E(log(ρ)) is the operative quantity to be maximized, rather than
168 E(ρ). Note that applying the log transformation has the effect of placing heavier penalties on fitness values
169 that are close to 0, so that maximizing mean log fitness will tend to encourage lower standard deviation
170 in fitness(25) (Figure 4C). This relationship between deviation in fitness and overall fitness again implies
171 bet-hedging behavior, supporting our hypothesis.

172

173 <u>Time intervals from ingestion of *C. neoformans* to initial budding are stochastic</u>

174 *C. neoformans* replication rate is highly dependent on pH(15). Consequently, we hypothesized that if
175 phagolysosomal acidification followed stochastic dynamics, this would be reflected on the time interval
176 from ingestion to initial replication. Analysis of time intervals to initial fungal cell budding events revealed
177 stochastic dynamics with no evidence of forbidden ordinal patterns (SFig 2B). Similar results were
178 observed for initial budding of wild type and urease negative strains of *C. neoformans*, which reside in
179 phagolysosomes that differ in final pH as a result of ammonia generation from urea hydrolysis.
180 Acidification intervals for both strains were stochastic, despite the fact that phagolysosomes of urease
181 deficient strains are approximately 0.5 pH units lower than those of wild type strains(15).

182

183 <u>Trained murine macrophages have inverse acidification dynamics</u>

184 Trained immunity has recently been shown to influence repeated infection in monocyte populations not
185 exposed to the adaptive immune system(26). To determine whether initial exposure to a pathogen has
186 an effect in the dynamics of this system we exposed BMDMs to *C. neoformans,* resolved the infection with
187 antifungals, and measured phagolysosome acidification dynamics upon reinfection. We found that pH
188 distribution of phagolysosomes from macrophages previously trained as described also exhibited
189 stochastic behavior (Figure 5A), veering away from a normal distribution of pH (Figure 5B and SFig 3,4).

However, trained BMDMs on average exhibited a significantly lower initial pH, which became significantly higher compared to untrained BMDMs over time (Figure 5C). Fully understanding this system will require significant further study outside the scope of this manuscript. In this regard we note that amphotericin B is a powerful activator of macrophages(27) and that *C. neoformans* residence inside macrophages is associated with host cell damage(28, 29). Hence, the effects we observe could be the aggregate of several influences in the system. Nevertheless, there is a clear suggestion of a historical effect on which pH distribution a macrophage will employ. This may also suggest an adaptive component to the macrophage bet-hedging strategy.

Human monocytes acidify stochastically and approximate normality

To determine how closely the murine system resembled human acidification dynamics, we isolated macrophages from human peripheral blood monocytes and repeated these experiments with beads and live *C. neoformans*. We found that acidification intervals in human cells were also stochastic in nature (Figure 6A). Additionally, human cells that ingested inert beads were normally distributed at the 15 min and 1 h time intervals. Even though the times skewed away from normality, the skew was not as severe as that observed in yeast containing phagolysosomes (Figure 6B). We hypothesize that some of this skewing could result from different dynamics due to the different background inherent to human donors, which differ from the mouse system in which cells are isolated from genetically identical individuals (SFig 5). Furthermore, within the context of our simulation, if we model the phagolysosome pH values of a population of human macrophages as a normal distribution with mean and standard deviation determined from pH values observed across all time points (5.08 and 1.08, respectively), the resulting mean log fitness is high with dramatically reduced deviation in fitness (Figure 4).

Cryptococcus neoformans skews phagolysosome acidification towards conditions favorable to the yeast

Cryptococcal cells buffer the phagolysosome pH toward 5.5, a value optimal for yeast growth(14). We therefore hypothesized that *C. neoformans* could use this buffering capability to disrupt the host acidification strategy. We found that phagolysosomes containing live *C. neoformans* and live *C. gattii* acidified to distributions of pH less normally distributed and more permissive to general fungal replication by increasing the average observed phagolysosomal pH.

To probe host fitness with regard to *C. neoformans* specifically, we modified our model by declaring the inhibitory pH as ≤ 4, which inhibits *C. neoformans* replication(30), and calculated the likelihood of each population of macrophages to achieve an inhibitory pH, assuming phagolysosome pHs were normally distributed around the observed mean and standard deviation. Here we analyzed the combined data for all time intervals, reasoning that in actual infection interactions between *C. neoformans* and host macrophages early phagosomes would be important as well, rather than focusing only on mature phagolysosomes.

226 We estimated the proportions of inhibitory phagolysosomes and found that bead-containing
227 phagolysosomes were more likely to acidify to ≤ 4, followed by heat-killed and *Δure1 C. neoformans*,
228 followed by live *C. neoformans*, with capsule deficient *Cap59* being particularly likely, and trained
229 macrophages or *C. gattii* containing phagolysosomes being particularly unlikely to achieve inhibitory pH
230 (Fig 7A). Our actual data was not normally distributed with non-bead samples though, as *C. neoformans*
231 actively modulates phagolysosomal pH. The starkest difference we observed is that killed and live *C.*
232 *neoformans* phagolysosomes had the same proportion of inhibitory phagolysosomes, suggesting the
233 capsule has a more significant effect on pH modulation than we initially expected. This finding is
234 corroborated by the high proportion of inhibitory phagolysosomes in *Cap59* containing phagolysosomes,
235 a strain incapable of modulating pH since it has no capsule (Fig 7C). Additionally, the expected and
236 observed increased likelihood of bead containing phagolysosomes to inhibit *C. neoformans* replication
237 compared to live *C. neoformans* phagolysosomes was consistent between murine and human cells (Fig
238 7B,D).

239

240 **Discussion**

241 The complexity and sequential nature of the phagolysosomal maturation process combined with the
242 potential for variability at each of the maturation steps, and the noisy nature of the signaling networks
243 that regulate this process, have led to the proposal that each phagolysosome is a unique and individual
244 unit(31). In fact, the action of kinesin and dynein motors that move phagosomes along microtubules
245 exhibits stochastic behavior, adding an additional source of randomness to the process(32). Hence, even
246 when the ingested particle is a latex bead taken through one specific type of phagocytic receptor there is
247 considerable heterogeneity in phagolysosome composition, even within a single cell(31). Since the
248 phagolysosome is a killing machine used to control ingested microbes, this heterogeneity implies there
249 will be differences in the microbicidal efficacy of individual phagolysosomes. This variability raises
250 fundamental questions about the nature of the dynamical system embodied in the process of phagosomal
251 maturation.

252

253 In this study, we analyzed the dynamics of phagolysosome pH variability after ingesting live yeast cells,
254 dead yeast cells, and latex particles. We sought to characterize the acidification dynamics as either
255 stochastic—an inherently unpredictable process with identical starting conditions yielding different
256 trajectories in time, or deterministic—a theoretically predictable process with identical starting conditions
257 leading to identical trajectories. In particular, we focused our analysis on differentiating stochastic vs.
258 chaotic signatures in the trajectories of phagolysosomal pH. While both dynamics might yield highly
259 divergent trajectories for similar starting conditions (i.e. only one of 100 variables differing by only a
260 minuscule amount), a chaotic system is inherently deterministic, such that if strictly identical starting
261 conditions were replicated, the same trajectory would follow from those conditions each time. A chaotic
262 system is defined as one so sensitive to initial conditions that, in practice, initial conditions cannot be
263 replicated precisely enough to see these same trajectories followed. The dynamical signatures of such
264 systems are unique and can be differentiated from that of deterministic or stochastic dynamics.

Irrespective of the nature of the ingested particle, we observed that the distribution of the increment of phagolysosomal pH reduction was random, indicative of a stochastic process. We found no evidence that phagosome acidification was a chaotic process. Systems in which a large number of variables each contribute to an outcome tend to exhibit 'noise', which gives them the characteristics of a stochastic dynamical system. In this regard, our finding that phagolysosomal pH demonstrates stochastic features is consistent with our current understanding of the mechanisms involved. Quantile-Quantile (Q-Q) plots revealed that most phagolysosomal pH distributions in this study manifested significant deviations from normality in several instances. The most normally distributed pH sets were those resulting from the ingestion of latex beads, particles that cannot modify the acidity of the phagolysosome. We note that for the three *C. gattii* strains the pH distributions revealed more skewing in Q-Q plots than for the H99 *C. neoformans* strain. Although the cause of this variation is not understood and the strain sample size is too small to draw firm conclusions, we note that such variation could reflect more microbial-mediated modification of the phagolysosomal pH by the *C. gattii* strains. In this regard, the capsular polysaccharide of *C. gattii* strains has polysaccharide triads that are more complex(33) and, given that the cryptococcal polysaccharide capsule contains glucuronic acids that can modify phagolysosomal pH via acid-base properties(17), it is possible that this skewing reflects differences in phagolysosome to phagosome capsular effects.

For most microbes, maintenance of an acidic environment in the phagolysosome is critically determinant on the integrity of the phagolysosomal membrane, keeping protons in the phagolysosomal lumen whilst excluding more alkaline cytoplasmic contents. For example, with *C. albicans,* the rupture of the phagolysosomal membrane is followed by rapid alkalization of the phagolysosomal lumen(34). For *C. neoformans*, phagolysosomal integrity is compromised by secretion of phospholipases that damage membranes as well as the physical stress on membranes resulting from capsular enlargement in the phagolysosome(14). However, for *C. neoformans*, loss of phagolysosomal membrane integrity does not immediately result in loss of phagolysosomal acidity, which is attributed to buffering by glucuronic acid residues in the *C. neoformans* capsule(17). Adding to the complexity of the *C. neoformans*-macrophage interaction is the fact that the phagolysosomal pH in the vicinity of 5.5 matches the optimal replication pH for this fungus(15), which can be expected to place additional stress on the organelle membrane through the increased volume resulting from budding cells. Treating macrophages with chloroquine, which increases phagosomal pH(35), potentiates macrophage antifungal activity against *C. neoformans*(36). Hence, phagosomal acidification does not inhibit *C. neoformans* replication but is critical for activation of mechanisms involved in antigen presentation(37). In the cryptococcal-containing phagolysosome the luminal pH is also likely to reflect a variety of microbial-mediated variables which include ammonia generation from urease, capsular composition, and the integrity of the phagolysosomal membrane.

303 Analysis of the normality of phagolysosomal pH distributions as a function of time by the Shapiro-Wilk
304 test produced additional insights into the dynamics of these systems. Phagolysosomes containing inert
305 beads manifested pH distributions that met criteria for normality at most time intervals after 1 h post
306 infection (HPI). We hypothesize that at 0.25 and 0.5 HPI there are two populations of phagolysosomes,
307 mature and maturing, with the latter having not yet fully acidified and thus resulting in the observed
308 bimodal distributions. In contrast, the pH distribution of phagolysosomes containing dead *C. neoformans*
309 cells initially veered away from normality at 15 min, 30 min, and 1 h but in later time intervals approached
310 normality, meeting the criteria for normality at 3 h. One interpretation of this result is that the process of
311 phagocytosis is itself a randomizing system with Gaussian noise resulting from phagolysosome formation
312 and kinetics of the initial acid-base reactions between increasing proton flux and quenching glucuronic
313 acids in the capsular polysaccharide. With time, the titration is completed as all glucuronic acid residues
314 are protonated, as dead cells did not synthesize additional polysaccharide, which moved the
315 phagolysosomal pH distribution towards normality. A similar effect may have occurred with strains R265,
316 W179, and *ure1Δ*. Convergence to or away from normality could reflect a myriad of such variables
317 affecting phagolysosomal pH including the intensity of acidification, the volume of the phagolysosome
318 (largely determined by the yeast capsule radius), the glucuronic acid composition of the capsule, the
319 production of ammonia by urease, and the leakiness of the phagolysosome to cytoplasmic contents with
320 higher pH. Although our experiments cannot sort out the individual contributions of these factors, they
321 suggest that, in combination, they produce Gaussian noise effects that push or pull the resulting
322 distribution to or from normality. Additionally, human phagolysosome acidification dynamics resembled
323 those of mouse cells but noted significant differences in the distributions of phagolysosomal pH between
324 individual human donors. This donor-to-donor variation could reflect differences in polymorphisms in Fc
325 receptor genes or other genetic variables and is an interesting subject for future studies.

326

327 When a phagocytic cell ingests a microbe, it has no information as to the pH range tolerated by the
328 internalized microbe. A stochastic dynamical process for phagolysosomal acidification could provide
329 phagocytic immune cells and their hosts with the best chance for controlling ingested microbes. The acidic
330 pH in the phagolysosome activates microbicidal mechanisms and acidity is not generally considered a
331 major antimicrobial mechanism in itself. However, our analysis of pH tolerances of 27 pathogenic
332 microbes revealed that the majority are inhibited by phagolysosomal pH with the caveat that some, like
333 *C. neoformans*(18) and *Salmonella typhimrium*(38), thrive in acidified phagolysosomes. On the other hand,
334 a less acidic phagosomal pH is conducive to intracellular survival for *M. tuberculosis*(39). During an
335 infectious process when the immune system confronts numerous microbial cells the random nature of
336 the final phagosomal pH will result in some fraction of the infecting inoculum being controlled, and
337 possibly killed, by initial ingestion allowing antigen presentation. In this regard, the mean number of
338 bacteria in the phagolysosomes and cytoplasm of macrophages infected with the intracellular pathogen
339 *Franciscella tularensis* exhibits stochastic dynamics(40), which in turn could result from the type of
340 stochastic processes in phagolysosome formation noted here. Hence, chance in phagolysosomal pH
341 acidification provides phagocytic cells with a mechanism to hedge their bets such that the stochastic
342 nature of the process is itself a host defense mechanism.

In biology, bet-hedging was described by Darwin as a strategy to overcome an unpredictable environment(41), which is now known as diversified bet-hedging: diversifying offspring genotype to ensure survival of at least some individuals at the expense of reducing the mean inclusive fitness of the parent. The main idea behind any bet-hedging strategy, under the assumption of multiplicative fitness, is that to maximize long-term fitness, an organism must lower its variance in fitness between generations(42–44). For example, varying egg size and number in a clutch can bank against years with a hostile environment in a form of diversified bet-hedging(45). During any given "good year" fewer of the offspring will thrive because some are specifically designated for survival in "bad years", drastically increasing fitness during bad years at the cost of a slight fitness reduction during good. Our observations suggest that, as a population, macrophages perform a bet-hedging strategy by introducing a pH level as inhospitable to pathogens as possible, while still maintaining biologically possible levels. However, such an approach could select for acid-resistant microbes. Our observation suggests that to avoid an arms-race, the macrophage not only lowers the pH level to a level that is unfavorable to most microbes, since the reduction in pH level reduces the optimal growth condition to around 70% of the optimum (see Figure 3 red line under the blue shaded curve), but it also introduces randomness in the achieved pH, such that ingested microbes are less likely to adapt to the potentially hostile environment. In other words, tightly controlled pH reduction by the host without increased variation, might introduce an evolutionary arm-race between pathogens and their host cells, leading towards deleterious outcome of selecting microbial acid resistance. Additionally, our model shows that even at the lower extreme mean pH, macrophage populations still benefit in the long run by increasing their phagolysosomal pH. We note that the pH of other mammalian fluids such as that of the blood are tightly regulated such that their physiological variance is very small(46). For example, human plasma pH averages 7.4 with a range of only 0.05 units. Hence, organisms can maintain tight pH control when it is physiologically important, thus implying that the comparatively large range of phagolysosomal pHs measured in all conditions studied is a designed feature of this system. In other words, one can envision the macrophage's first line of defense of bet-hedging phagolysosomal pH as a roulette wheel, where the payout is likelihood of macrophage survival and the placed bet is a range of possible pH. Placing multiple bets across the table (increasing standard deviation of pH distribution) increases the chance of winning at the cost of a lower payout (mean fitness), resulting in a more profitable long-term strategy (increased mean log fitness). In fact, the most profitable roulette strategy is broad color bets with lower payouts but the best winning probability. The most profitable betting strategy would of course be to play Blackjack instead, but macrophages do not have that luxury.

Given that acid has potent antimicrobial properties, one might wonder why phagolysosomal acidification does not reach even lower and more acidic pHs. There are several explanations for observed lower limits in pH. Acidification is achieved by pumping protons into the vacuole and achieving lower pHs against an ever-increasing acidity gradient could prove thermodynamically difficult. There is also evidence that the integrity of the cell membrane lipid bilayer is compromised by acidity at pHs of 3 and below(47, 48) which could promote leakage of phagolysosomal contents into the cytoplasm with damage to the host cell.

383 Consequently, we propose that a larger variation in macrophage phagolysosomal pH acts as a diversified
384 bet-hedging strategy against the stochasticity of the potential pH tolerances of ingested microbes within
385 the physiological limits of achievable acidification. This hypothesis is supported by simulated data in which
386 an increase in standard deviation of the pH distribution slightly lowers the expected mean but significantly
387 decreases the standard deviation of host survival. Fully analyzing the consequences and evolutionary
388 tradeoff of this strategy would require a closer analysis that considers the costs and benefits with regard
389 to the host. Though outside the scope of our current work, our observations suggest this line of
390 investigation for future studies.

391

392 Our results delineate new avenues for investigation. Most perplexing is how a random phagolysosomal
393 pH is established and maintained. One can imagine various mechanisms including variation in the number
394 of ATPase molecules and/or differences in activity of individual pumps depending on location and
395 adjoining structures. To resolve this would require sophisticated technology allowing the measurement
396 of pH in individual phagolysosomes as a function of pump occupancy and efficacy. Such techniques are
397 likely beyond the current technological horizon but suggests new fertile areas of scientific investigation.
398 From a clinical perspective, a drug that increases variation in phagolysosomal pH could be useful in
399 enhancing macrophage anti-microbial efficacy in situations which one cannot anticipate which specific
400 microbes will be encountered. On the other hand, drugs that specifically modulate pH may be useful in
401 situations with specific microbes that express marked acid/base tolerance. In this regard, chloroquine
402 alkalizes *C. neoformans* phagolysosomes, moving away from optimal inhibitory pH. This drug has been
403 shown to enhance macrophage activity against *C. neoformans*(9, 49).

404

405 In summary, we document that phagolysosomal acidification, a critical process for phagocytic cell efficacy
406 in controlling ingested microbial cells, manifests stochastic dynamics that permit a bet-hedging strategy
407 for phagocytic cells ingesting microbes of unknown pH tolerance. These observations establish that the
408 use of bet-hedging strategies in biology extends to the sub-organism level to involve cells and their
409 organelles. This, in turn, implies a significant role for chance in the resolution of conflict between microbes
410 and host phagocytic cells in individual phagolysosomes. We have recently argued that chance is also a
411 major determinant of individual susceptibility to infectious diseases at the organismal level(50). Variability
412 in the outcome of infectious disease between individual hosts may reflect the sum of innumerable chance
413 events for host-microbe interactions at the cellular level, which include the process of phagosome
414 acidification.

415

416 **Methods**

417 <u>Cell Strains and Culture Conditions</u>

418 *Cryptococcus gattii* species complex strains R265, WM179, and WM161 were obtained from ATCC
419 (Manassas, VA), and *Cryptococcus neoformans* species complex serotype A strain H99 as well as *ure1Δ*

420 (lacking urease, derived from H99) were originally obtained from John Perfect (Durham, NC). The strains
421 were stored at 80°C.Frozen stocks were streaked onto Sabouraud dextrose agar (SAB) and incubated at
422 30°C. Liquid suspensions of cryptococcal cultures were grown in SAB overnight at 30°C. Cryptococcal
423 cultures were heat killed by incubating at 65 °C for 1 h.

424 Macrophage cells were either mouse bone marrow-derived macrophages (BMDM) obtained from 6 week
425 old C57BL/6 female mice from The Jackson Laboratory (Bar Harbor, ME), J774.16 macrophage-like cells,
426 or human monocytes isolated from PMBCs. BMDMs were isolated from hind leg bones and for
427 differentiation were seeded in 10 cm tissue culture treated dishes (Corning, NY) in Dulbecco's Modified
428 Eagle Medium (DMEM, Corning) with 10% FBS (Atlanta Biologicals, Flowery Branch, GA), 1% nonessential
429 amino acids (Cellgro, Manassas, VA), 1% penicillin-streptomycin (Corning), 2 mM Glutamax (Gibco,
430 Gaithersburg, MD), 1% HEPES buffer (Corning), 20% L-929 cell conditioned supernatant, 0.1% beta-
431 mercaptoethanol (Gibco) for 6 days at 37 °C and 9.5% CO_2. BMDMs were used for experiments within 5
432 days after differentiation. J774.16 cells were cultured in DMEM with 10% FBS, 1% nonessential amino
433 acids, 10% NCTC109 (Gibco), and 1% penicillin-streptomycin at 37 °C with 9.5% CO_2. For human peripheral
434 blood mononuclear cells (hPBMCs), CD14+ monocytes were isolated using Dynabeads Untouched Human
435 Monocytes Kit (Thermo Fisher Scientific) according to the manufacturer protocol. The isolated cells were
436 differentiated in RPMI-1640 medium (RPMI) with 10% FBS (Atlanta Biologicals, Flowery Branch, GA), 1%
437 penicillin-streptomycin (Corning), and 25 ng/mL of human granulocyte-macrophage colony-stimulating
438 factor (GM-CSF, Sigma-Aldrich) for five days. Human cells were further cultured in RPMI (RPMI) with 10%
439 FBS (Atlanta Biologicals, Flowery Branch, GA), 1% penicillin-streptomycin (Corning), and activated with 0.5
440 ug/mL LPS and 10 ng/mL IFN-γ.

441

442 Phagolysosomal pH measurement

443 Phagolysosomal pH was measured using ratiometric fluorescence imaging involving the use of pH-
444 sensitive probe Oregon green 488 as described in prior studies(15). The pH values analyzed here were
445 collected in part during prior studies of *C. neoformans*-macrophage interactions(14–16). Briefly, Oregon
446 green 488 was first conjugated to monoclonal antibody (mAb) 18B7, which binds *C. neoformans* capsular
447 polysaccharide, using Oregon Green 488 Protein Labeling Kit (Molecular Probes, Eugene, OR). The labeling
448 procedure was done by following the manufacture's instruction. BMDMs were plated at a density of 1.25
449 × 10^5 cells/well or differentiated human macrophages were plated at a density of 2.5 x 10^5 cells/well on
450 24-well plate with 12 mm circular coverslip. Cells were activated with 0.5 µg/ml lipopolysaccharide (LPS;
451 Sigma-Aldrich) and 100 U/ml interferon gamma (IFN-γ; Roche), at 37 °C in a 9.5% CO_2 (BMDM) or 5% CO_2
452 (Human macrophage) atmosphere overnight. Prior to infection, 2 d old live, heat killed H99, R265,
453 WM179, ure1, cap59, or anti-mouse IgG coated polystyrene bead (3.75 × 10^6 cells or beads/ml) were
454 incubated with 10 µg/ml Oregon green conjugated mAb 18B7 for 15 min. Macrophages were then
455 incubated with Oregon green conjugated mAb 18B7-opsonized particles in 3.75 × 10^5 cryptococcal cells
456 or beads per well (BMDM) or 2.5 x 10^5 cell/well (Human macrophage). Cells were centrifuged immediately
457 at 350 x g for 1 min to synchronize ingestion and cultures were incubated at 37 °C for 10 min to allow
458 phagocytosis. Extracellular cryptococcal cells or beads were removed by washing three times with fresh
459 medium, a step that prevents the occurrence of new phagocytic events. As an additional safeguard against

460 new phagocytic events fresh media was supplemented with AlexaFluor 568 conjugated mAb 18B7 for 1 h
461 to label extracellular particles. Samples on coverslip were collected at their respective time points after
462 phagocytosis by washing twice with pre-warmed HBSS and placing upside down on MatTek petri dish
463 (MatTek, Ashland, MA) with HBSS in the microwell. Images were taken by using Olympus AX70 microscopy
464 (Olympus, Center Valley, PA) with objective 40x at dual excitation 440 nm and 488 nm, and emission 520
465 nm. Images were analyzed using MetaFluor Fluorescence Ratio Imaging Software (Molecular Devices,
466 Downingtown, PA). Fluorescence intensities were used to determine the ratios of Ex488 nm/Ex440 nm
467 that were converted to absolute pH values using a standard curve where the images are taken as above
468 but intracellular pH of macrophages was equilibrated by adding 10 µM nigericin in pH buffer (140 mM KCl,
469 1 mM $MgCl_2$, 1 mM $CaCl_2$, 5 mM glucose, and appropriate buffer ≤ pH 5.0: acetate-acetic acid; pH 5.5-6.5:
470 MES; ≥ pH 7.0: HEPES. Desired pH values were adjusted using either 1 M KOH or 1 M HCl). The pH of
471 buffers was adjusted at 3-7 using 0.5-pH unit increments.

472

473 Trained macrophage experiments

474 BMDMs were plated at a density of 2×10^5 cells/well on 24-well plate with 12 mm circular coverslip.
475 Cells were activated with 0.5 µg/ml LPS and 100 U/ml IFN-γ; Roche and incubated at 37 °C in a 9.5% CO_2
476 atmosphere overnight. Prior to the infection, H99 were stained with 0.01% Uvitex 2B for 10 min.
477 BMDMs were then infected with H99 (2×10^5 cells/well) in the presence of 10 µg/ml 18B7. After 1 h of
478 infection, 5 µg/ml of amphotericin B were added to each well and the culture were incubated for
479 overnight. On the following day, the cultures were washed three times with PBS, and incubated in PBS
480 for 2 h. After the incubation, the cultures were further washed three times with PBS. A fresh overnight
481 culture of H99 were incubated with 10 µg/ml Oregon green conjugated mAb 18B7 for 15 min.
482 Macrophages were then incubated with Oregon green conjugated mAb 18B7-opsonized H99 in 2×10^5
483 cells per well. Cells were centrifuged immediately at 350 x g for 1 min to synchronize ingestion.
484 Phagolysosomal pH were then measured using Olympus AX70 microscopy.

485

486 Time-lapse imaging and intracellular replication

487 The time of intracellular replication here were collected in time-lapse imaging during prior studies of *C.*
488 *neoformans*-macrophage interactions(15). For imaging BMDM (5×10^4 cells/well) were plated on poly-D-
489 lysine coated coverslip bottom MatTek petri dishes with 14mm microwell (MatTek). Cells were cultured
490 in completed DMEM medium and stimulated with 0.5 µg/ml LPS and 100 U/ml IFN-γ overnight at 37 °C
491 with 9.5 % CO_2. On the following day, macrophages were infected with cryptococcal cells (H99 or ure1;
492 1.5×10^5 cells/well) opsonized with 18B7 (10 µg/ml). After 2 h incubation to allow phagocytosis,
493 extracellular cryptococcal cells were removed by washing the culture five times with fresh medium.
494 Images were taken every 4 min for 24 h using a Zeiss Axiovert 200M inverted microscope with a 10x phase
495 objective in an enclosed chamber at 9.5 % CO_2 and 37 °C. The time intervals to initial replication of
496 individual cryptococcal cells inside macrophage were measured in time-lapse imaging.

497

498 Data Processing

499 Phagolysosome pH intervals were calculated by subtracting measured pH levels of phagolysosomes from
500 a starting pH of 7.2, and individual interval measurements were concatenated into a single dataset for
501 each time point examined.

502

503 Data analysis

504 Discrimination of deterministic vs. stochastic dynamics was achieved using the previously characterized
505 permutation spectrum test(21). In this method, the processed datasets were segmented into overlapping
506 subsets of 4 data points using a sliding window approach, as detailed in figure 4, and assigned 1 of 24 (4!)
507 possible ordinal patterns based on the ordering of the 4 terms in the subset. The frequencies with which
508 each unique ordinal pattern occurred in the dataset were then calculated and plotted. Deterministic
509 dynamics were characterized by the occurrence of "forbidden ordinals", equal to ordinal patterns that
510 doesn't occur in the dataset whereas stochastic dynamics were characterized by the presence of all
511 ordinals. Measured phagolysosomal pHs were subtracted from an initial pH value (7.2) based on cell media
512 pH and placed in a vector. Subsets of 4 data points were generated using a sliding window approach in
513 which the first four values were grouped, the window shifted by one, and the subsequent set of 4 values
514 grouped. Each subset was prescribed an "ordinal pattern" based on the relative values of the data points
515 in the subset to each other with, for instance, the lowest value assigned a "0" in the ordinal pattern and
516 the highest a "3". Further characterization of deterministic dynamics was achieved using the previously
517 characterized point count plot(51), in which periodic vs. chaotic dynamics were differentiated based on
518 the distribution of "peaks" in the calculated power spectrum of each dataset. Power spectrums were
519 estimated with Matlab's Lomb-Scargle power spectral density (PSD) estimate function and subsequently
520 normalized. From the normalized power spectrum, "point count plots" were generated by counting the
521 number of peaks above a set threshold—the point threshold—with values of the point threshold ranging
522 from 0 to 1. Periodic dynamics were characterized by "staircase" point count plots whereas chaotic
523 dynamics were characterized by point count plots with a decreasing exponential shape.

524

525 Distribution and normality analysis

526 Each set of sample data was fit to a series of distributions using the R package "fitdistrplus" with default
527 parameters for each distribution type, generating the histograms and Quantile-Quantile (Q-Q) plots.
528 Normality and significance were calculated via the base R Shapiro-Wilk test.

529

530 Generating and Analyzing Simulations

531 Let f(x) be the probability distribution of the host's pH. For simplicity, we assume that f is Normal(μ, σ).
532 Let F(x) be the corresponding cdf. At every time-point, we randomly sample a pathogen i from a set of
533 pathogens. The pathogen has a range (a_i, b_i) of viable pH, which differs among pathogens. Minimum

534 tolerable pH values were obtained from the literature as described, while a constant value of 8 was used
535 for maximum since most pathogens were inhibited as high pH as well as phagolysosomes being unlikely
536 to alkalize. The host, in turn, randomly chooses a pH by sampling from the distribution f(x). If the host's
537 pH x falls in the interval (a_i,b_i), then there is a probability p of the host dying. We can think of the host's
538 survival rate ρ as its fitness, which is a random variable that depends on the randomness in pathogens. As
539 a function of i, we have ρ(i)=p*(F(b_i)-F(a_i)); the random variable ρ assumes the values ρ(i) with equal
540 probability.

541

542 **Author Contributions**

543 Conceptualization, Q.D., K.S., A.V, A.C; Methodology: Q.D., K.S., Y.S., M.F., Y.S., C.Y., A.B., A.C.; Software,
544 Q.D., K.S., Y.S., A.V.; Formal Analysis, Q.D.; Investigation, Q.D., K.S., Y.S., M.F., Y.S., C.Y., I.Y., C.M.DLR, J.F.,
545 A.B., A.C.; Writing – Original Draft, Q.D., K.S., M.F, A.B., A.C.; Writing – Review & Editing, Q.D., K.S., Y.S.,
546 M.F., Y.S., C.Y., I.Y., C.M.DLR, J.F., A.B., A.C.; Visualization, Q.D.

547

548 **Acknowledgements**

549 Arturo Casadevall was supported by grants R01HL059842, 5R01AI033774, 5R37AI033142, and
550 5R01AI052733. Quigly Dragotakes is supported by a fellowship from the Achievement Rewards for College
551 Scientists (ARCS) Foundation Metro-Washington Chapter as well as a National Institutes of Health T32.

552

553 **References**

554 1. Broderick NA. A common origin for immunity and digestion. *Front Immunol* 2015;6:72.

555 2. Rosales C, Uribe-Querol E. Phagocytosis: A Fundamental Process in Immunity. *Biomed Res Int*
556 2017;2017:9042851.

557 3. Sun-Wada GH, Tabata H, Kawamura N, Aoyama M, Wada Y. Direct recruitment of H+-ATPase from
558 lysosomes for phagosomal acidification. *J Cell Sci* 2009;122(Pt 14):2504–2513.

559 4. Kinchen JM, Ravichandran KS. Phagosome maturation: going through the acid test. *Nat Rev Mol Cell*
560 *Biol* 2008;9(10):781–795.

561 5. Jankowski A, Scott CC, Grinstein S. Determinants of the phagosomal pH in neutrophils. *J Biol Chem*
562 2002;277(8):6059–6066.

563 6. Bouvier G, Benoliel AM, Foa C, Bongrand P. Relationship between phagosome acidification,
564 phagosome-lysosome fusion, and mechanism of particle ingestion. *J Leukoc Biol* 1994;55(6):729–734.

565 7. Geisow MJ, D'Arcy Hart P, Young MR. Temporal changes of lysosome and phagosome pH during
566 phagolysosome formation in macrophages: studies by fluorescence spectroscopy. *J Cell Biol*
567 1981;89(3):645–652.

568 8. Feldmesser M, Kress Y, Novikoff P, Casadevall A. Cryptococcus neoformans is a facultative intracellular

569 pathogen in murine pulmonary infection [Internet]. *Infect. Immun.* 2000;68(7):4225–4237.

570 9. Levitz SM et al. Cryptococcus neoformans resides in an acidic phagolysosome of human macrophages
571 [Internet]. *Infect. Immun.* 1999;67(2):885–890.

572 10. Ma H, Croudace JE, Lammas DA, May RC. Expulsion of Live Pathogenic Yeast by Macrophages
573 [Internet]. *Curr. Biol.* 2006;16(21):2156–2160.

574 11. Alvarez M, Casadevall A. Phagosome fusion and extrusion, and host cell survival following
575 Cryptococcus neoformans phagocytosis by macrophages. *Curr. Biol.* 2006;16:2161–2165.

576 12. Ma H, Croudace JE, Lammas DA, May RC. Direct cell-to-cell spread of a pathogenic yeast [Internet].
577 *BMC Immunol.* 2007;8(1):15.

578 13. Alvarez M, Casadevall A. Cell-to-cell spread and massive vacuole formation after Cryptococcus
579 neoformans infection of murine macrophages [Internet]. *BMC Immunol.* 2007;8:16.

580 14. De Leon-Rodriguez CM et al. The Outcome of the *Cryptococcus neoformans*– Macrophage
581 Interaction Depends on Phagolysosomal Membrane Integrity [Internet]. *J. Immunol.* 2018;201(2):583–
582 603.

583 15. Fu MS et al. Cryptococcus neoformans urease affects the outcome of intracellular pathogenesis by
584 modulating phagolysosomal pH [Internet]. *PLOS Pathog.* 2018;14(6):e1007144.

585 16. Freij JB et al. Conservation of Intracellular Pathogenic Strategy among Distantly Related Cryptococcal
586 Species [Internet]. *Infect. Immun.* 2018;86(7). doi:10.1128/IAI.00946-17

587 17. De Leon-Rodriguez CM, Fu MS, Corbali MO, Cordero RJB, Casadevall A. The Capsule of Cryptococcus
588 neoformans Modulates Phagosomal pH through Its Acid-Base Properties. *mSphere* 2018;3(5).
589 doi:10.1128/mSphere.00437-18

590 18. DeLeon-Rodriguez CM, Casadevall A. Cryptococcus neoformans: Tripping on Acid in the
591 Phagolysosome [Internet]. *Front. Microbiol.* 2016;7:164.

592 19. Smith LM, Dixon EF, May RC. The fungal pathogen *C ryptococcus neoformans* manipulates
593 macrophage phagosome maturation [Internet]. *Cell. Microbiol.* 2015;17(5):702–713.

594 20. Davis MJ et al. Cryptococcus neoformans-induced macrophage lysosome damage crucially
595 contributes to fungal virulence. *J Immunol* 2015;194(5):2219–2231.

596 21. Zunino L, Soriano MC, Rosso OA. Distinguishing chaotic and stochastic dynamics from time series by
597 using a multiscale symbolic approach [Internet]. *Phys. Rev. E. Stat. Nonlin. Soft. Matter Phys* 2012;86(4
598 Pt 2):46210.

599 22. Fierer N, Jackson RB. The diversity and biogeography of soil bacterial communities. *Proc Natl Acad*
600 *Sci U S A* 2006;103(3):626–631.

601 23. Baath K. E ;Arnebrand. Growth rate and response of bacterial communities to pH in limed and ash
602 treated forest soils. *Soil Biol. Biochem.* 1994;26(8):995–1001.

603 24. Baath E, Frostegard A, Fritze H. Soil Bacterial Biomass, Activity, Phospholipid Fatty Acid Pattern, and
604 pH Tolerance in an Area Polluted with Alkaline Dust Deposition. *Appl Env. Microbiol* 1992;58(12):4026–
605 4031.

606 25. Karlin S, Lieberman U. Random temporal variation in selection intensities: case of large population

607 size. [Internet]. *Theor. Popul. Biol.* 1974;6(3):355–82.

608 26. Quintin J et al. Candida albicans infection affords protection against reinfection via functional
609 reprogramming of monocytes. [Internet]. *Cell Host Microbe* 2012;12(2):223–32.

610 27. Sau K et al. The Antifungal Drug Amphotericin B Promotes Inflammatory Cytokine Release by a Toll-
611 like Receptor- and CD14-dependent Mechanism [Internet]. *J. Biol. Chem.* 2003;278(39):37561–37568.

612 28. Casadevall A, Coelho C, Alanio A. Mechanisms of Cryptococcus neoformans-Mediated Host Damage.
613 *Front Immunol* 2018;9:855.

614 29. Coelho C et al. Macrophage mitochondrial and stress response to ingestion of Cryptococcus
615 neoformans [Internet]. *J. Immunol. (Baltimore, Md. 1950)* 2015;194(5):2345–2357.

616 30. Alspaugh JA, Granger DL. Inhibition of Cryptococcus neoformans replication by nitrogen oxide
617 supports the role of these molecules as effectors of macrophage-mediated cystostasis. *Infect. Immun*
618 1991;59:2291–2296.

619 31. Griffiths G. On phagosome individuality and membrane signalling networks. *Trends Cell Biol*
620 2004;14(7):343–351.

621 32. Mallik KCB, Banerjee PL, Chatterjee BD, Pramanick M. An experimental study of the course of
622 infection in mice after intranasal insufflation with Cryptococcus neoformans. *Ind. J. Med. Res*
623 1966;54:608–610.

624 33. Cherniak R, Valafar H, Morris LC, Valafar F. Cryptococcus neoformans chemotyping by quantitative
625 analysis of 1H NMR spectra of glucuronoxylomannans using a computer simulated artificial neural
626 network. *Clin. Diagn. Lab. Immunol* 1998;5:146–159.

627 34. Westman J, Moran G, Mogavero S, Hube B, Grinstein S. Candida albicans Hyphal Expansion Causes
628 Phagosomal Membrane Damage and Luminal Alkalinization. *MBio* 2018;9(5). doi:10.1128/mBio.01226-
629 18

630 35. Weber SM, Levitz SM. Chloroquine antagonizes the proinflammatory cytokine response to
631 opportunistic fungi by alkalizing the fungal phagolysosome. *J Infect Dis* 2001;183(6):935–942.

632 36. Harrison TS, Griffin GE, Levitz SM. Conditional lethality of the diprotic weak bases chloroquine and
633 quinacrine against Cryptococcus neoformans [Internet]. *J. Infect. Dis* 2000;182(1):283–289.

634 37. Artavanis-Tsakonas K, Love JC, Ploegh HL, Vyas JM. Recruitment of CD63 to Cryptococcus
635 neoformans phagosomes requires acidification [Internet]. *Proc. Natl. Acad. Sci. U. S. A*
636 2006;103(43):15945–15950.

637 38. Rathman M, Sjaastad MD, Falkow S. Acidification of phagosomes containing Salmonella typhimurium
638 in murine macrophages. *Infect Immun* 1996;64(7):2765–2773.

639 39. Queval CJ, Brosch R, Simeone R. The Macrophage: A Disputed Fortress in the Battle against
640 Mycobacterium tuberculosis. *Front Microbiol* 2017;8:2284.

641 40. Gillard JJ, Laws TR, Lythe G, Molina-Paris C. Modeling early events in Francisella tularensis
642 pathogenesis. *Front Cell Infect Microbiol* 2014;4:169.

643 41. Darwin C. *The Foundation of the Origin of Species: Two Essays Written in 1842 and 1844.* .
644 Cambridge, UK: Cambridge University Press; 1909:

645 42. Slatkin M. Cascading speciation. *Nature* 1974;252(5485):701–702.

646 43. Philippi T, Seger J. Hedging one's evolutionary bets, revisited. *Trends Ecol Evol* 1989;4(2):41–44.

647 44. Bergman A. TM. On the Natural Selection of Market Choice. *Auton. Agent. Multi. Agent. Syst.*
648 2002;5(4):387–395.

649 45. Olofsson H, Ripa J, Jonzén N. Bet-hedging as an evolutionary game: the trade-off between egg size
650 and number. [Internet]. *Proceedings. Biol. Sci.* 2009;276(1669):2963–9.

651 46. Curran RE et al. Control and Measurement of Plasma pH in Equilibrium Dialysis: Influence on Drug
652 Plasma Protein Binding [Internet]. *Drug Metab. Dispos.* 2011;39(3):551–557.

653 47. Leung C-Y et al. Crystalline polymorphism induced by charge regulation in ionic membranes.
654 [Internet]. *Proc. Natl. Acad. Sci. U. S. A.* 2013;110(41):16309–14.

655 48. Jacobsohn MK, Lehman MM, Jacobsohn GM. Cell membranes and multilamellar vesicles: Influence of
656 pH on solvent induced damage [Internet]. *Lipids* 1992;27(9):694–700.

657 49. Weber SM, Levitz SM, Harrison TS. Chloroquine and the fungal phagosome [Internet]. *Curr. Opin.*
658 *Microbiol.* 2000;3(4):349–353.

659 50. Casadevall A, Pirofski LA. What Is a Host? Attributes of Individual Susceptibility. *Infect Immun*
660 2018;86(2). doi:10.1128/iai.00636-17

661 51. Kulp CW, Zunino L. Discriminating chaotic and stochastic dynamics through the permutation
662 spectrum test. *Chaos* 2014;24(3):33116.

663 52. Zhan H et al. Kinetics and Novel Degradation Pathway of Permethrin in Acinetobacter baumannii ZH-
664 14. *Front Microbiol* 2018;9:98.

665 53. Raevuori M, Genigeorgis C. Effect of pH and sodium chloride on growth of Bacillus cereus in
666 laboratory media and certain foods. *Appl Microbiol* 1975;29(1):68–73.

667 54. Chenoweth MR, Somerville GA, Krause DC, O'Reilly KL, Gherardini FC. Growth characteristics of
668 Bartonella henselae in a novel liquid medium: primary isolation, growth-phase-dependent phage
669 induction, and metabolic studies. *Appl Env. Microbiol* 2004;70(2):656–663.

670 55. Tamimi HA, Hiltbrand W, Loercher H. Some growth requirements of Bacteroides fragilis. *J Bacteriol*
671 1960;80:472–476.

672 56. Venkatesh G.;Debral,A.K.;Kirpan,P.;Reers,M.;Murthy,P.V.V.S.;Swarupa,V.;Srikanth,L.;Sarma,P.V.G.K.
673 K ;Reine. pH Optimization and Production of High Potent Cellular Vaccine by Bordetella pertussis. *Int. J.*
674 *Biotechnol. Bioeng. Res.* 2012;3:17–25.

675 57. Brenner N.R.;Staley,J.T. DJ ;Krie. (ed). *Bergey's Manual of Bacteriology. The Proteobacteria*. New
676 York: Springer;

677 58. Jordan S.E. RC ;Jacob. The Effect of pH at Different Temperatures on the Growth of Bacterium coli
678 with a Constant Food Supply. *J.Gen.Microbiol.* 1948;2:15–24.

679 59. Silva J et al. Campylobacter spp. as a Foodborne Pathogen: A Review. *Front Microbiol* 2011;2:200.

680 60. Fisher K, Phillips C. The ecology, epidemiology and virulence of Enterococcus. *Microbiology*
681 2009;155(Pt 6):1749–1757.

682 61. Gera K, McIver KS. Laboratory growth and maintenance of Streptococcus pyogenes (the Group A
683 Streptococcus, GAS). *Curr Protoc Microbiol* 2013;30:Unit 9D.2.

684 62. Savic DJ, McShan WM. Long-term survival of Streptococcus pyogenes in rich media is pH-dependent.
685 *Microbiology* 2012;158(Pt 6):1428–1436.

686 63. Yang Q et al. The impact of pH and nutrient stress on the growth and survival of Streptococcus
687 agalactiae. *Antonie Van Leeuwenhoek* 2012;102(2):277–287.

688 64. Goodman NL, Larsh HW. Environmental factors and growth of Histoplasma capsulatum in soil.
689 *Mycopathol Mycol Appl* 1967;33(2):145–156.

690 65. Wadowsky RM, Wolford R, McNamara AM, Yee RB. Effect of temperature, pH, and oxygen level on
691 the multiplication of naturally occurring Legionella pneumophila in potable water. *Appl Env. Microbiol*
692 1985;49(5):1197–1205.

693 66. Tienungoon S, Ratkowsky DA, McMeekin TA, Ross T. Growth limits of Listeria monocytogenes as a
694 function of temperature, pH, NaCl, and lactic acid. *Appl Env. Microbiol* 2000;66(11):4979–4987.

695 67. Conner DE, Brackett RE, Beuchat LR. Effect of temperature, sodium chloride, and pH on growth of
696 Listeria monocytogenes in cabbage juice. *Appl Env. Microbiol* 1986;52(1):59–63.

697 68. Piddington DL, Kashkouli A, Buchmeier NA. Growth of Mycobacterium tuberculosis in a defined
698 medium is very restricted by acid pH and Mg(2+) levels. *Infect Immun* 2000;68(8):4518–4522.

699 69. Oh YK, Straubinger RM. Intracellular fate of Mycobacterium avium: use of dual-label
700 spectrofluorometry to investigate the influence of bacterial viability and opsonization on phagosomal pH
701 and phagosome-lysosome interaction. *Infect Immun* 1996;64(1):319–325.

702 70. Portaels F, Pattyn SR. Growth of mycobacteria in relation to the pH of the medium. *Ann Microbiol*
703 1982;133(2):213–221.

704 71. Pettit RK, McAllister SC, Hamer TA. Response of gonococcal clinical isolates to acidic conditions. *J*
705 *Med Microbiol* 1999;48(2):149–156.

706 72. Brookes R, Sikyta B. Influence of pH on the growth characteristics of Neisseria gonorrhoeae in
707 continuous culture. *Appl Microbiol* 1967;15(2):224–227.

708 73. Kohman EF. The So-called Reduced Oxygen Tension for Growing the Meningococcus. *J Bacteriol*
709 1919;4(6):571–584.

710 74. Tsuji A, Kaneko Y, Takahashi K, Ogawa M, Goto S. The effects of temperature and pH on the growth
711 of eight enteric and nine glucose non-fermenting species of gram-negative rods. *Microbiol Immunol*
712 1982;26(1):15–24.

713 75. Stokes JL, Bayne HG. Growth rates of Salmonella colonies. *J Bacteriol* 1957;74(2):200–206.

714 76. Valero A et al. Modelling the growth boundaries of Staphylococcus aureus: Effect of temperature, pH
715 and water activity. *Int J Food Microbiol* 2009;133(1–2):186–194.

716 77. Dernby KG, Avery OT. THE OPTIMUM HYDROGEN ION CONCENTRATION FOR THE GROWTH OF
717 PNEUMOCOCCUS. *J Exp Med* 1918;28(3):345–357.

718 78. Williams RP, Gott CL, Qadri SM, Scott RH. Influence of temperature of incubation and type of growth
719 medium on pigmentation in Serratia marcescens. *J Bacteriol* 1971;106(2):438–443.

720 79. Giri A V, Anandkumar N, Muthukumaran G, Pennathur G. A novel medium for the enhanced cell
721 growth and production of prodigiosin from Serratia marcescens isolated from soil. *BMC Microbiol*
722 2004;4:11.

723 80. Erlandson Jr. AL, Mackey WH. Nutrition of Shigella: growth of Shigella flexneri in a simple chemically
724 defined medium. *J Bacteriol* 1958;75(3):253–257.

725 81. Patel M.;Gouws,E. M ;Isaacso. Effect of Iron and pH on the survival of Vibrio cholerae in water.
726 *Trans. R. Soc. Trop. Med. Hygene* 1995;89:175–177.

727 82. Huq A, West PA, Small EB, Huq MI, Colwell RR. Influence of water temperature, salinity, and pH on
728 survival and growth of toxigenic Vibrio cholerae serovar 01 associated with live copepods in laboratory
729 microcosms. *Appl Env. Microbiol* 1984;48(2):420–424.

730 83. Adams MR, Little CL, Easter MC. Modelling the effect of pH, acidulant and temperature on the
731 growth rate of Yersinia enterocolitica. *J Appl Bacteriol* 1991;71(1):65–71.

732 84. Brubaker RR. Influence of Na(+), dicarboxylic amino acids, and pH in modulating the low-calcium
733 response of Yersinia pestis. *Infect Immun* 2005;73(8):4743–4752.

734 85. Perry RD, Fetherston JD. Yersinia pestis--etiologic agent of plague [Internet]. *Clin. Microbiol. Rev*
735 1997;10(1):35–66.

736

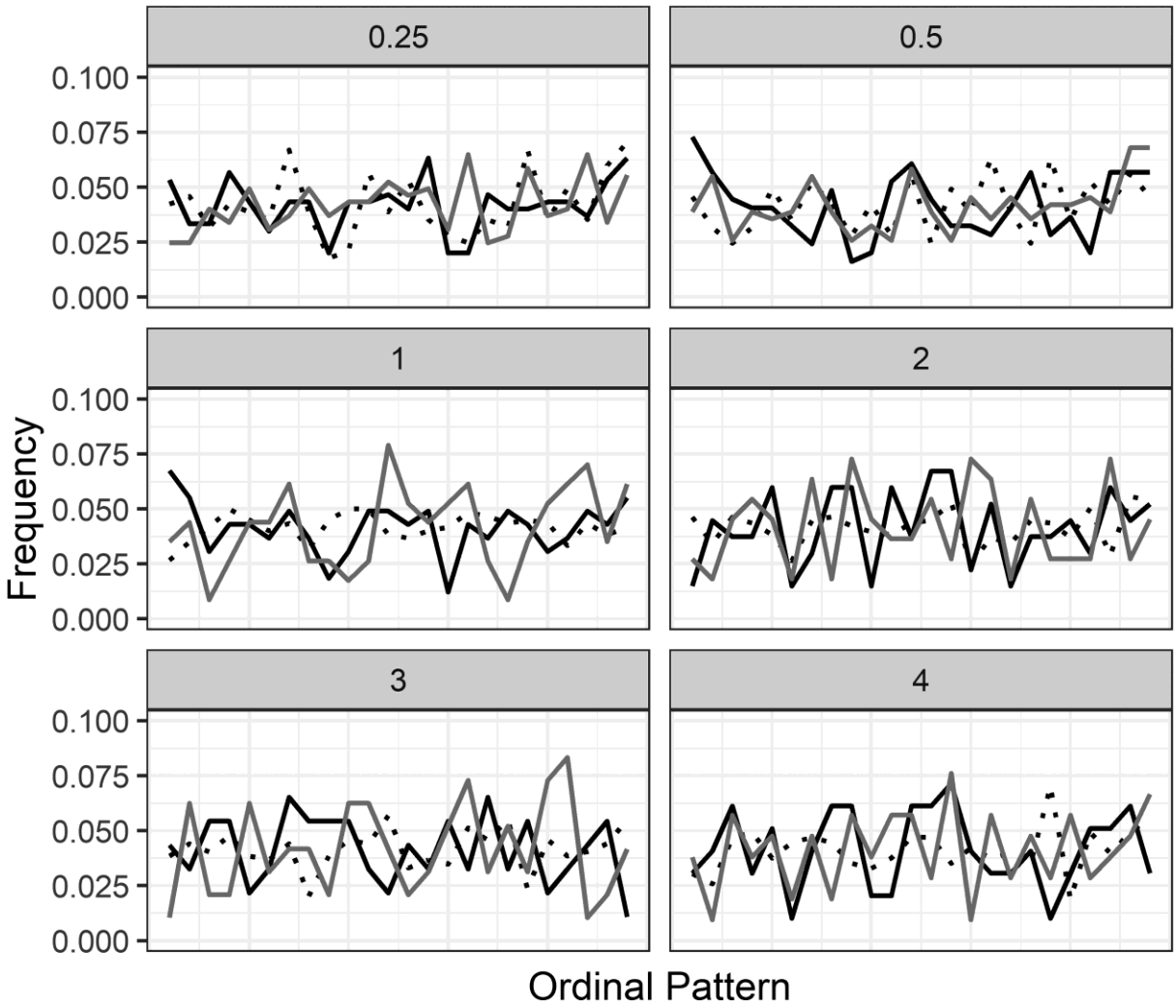

Figure 1. Murine macrophage phagolysosomes acidify stochastically. The frequency of each 4-unit ordinal pattern for each ingested particle: beads (solid black), live *C. neoformans* (dotted), and dead *C. neoformans* (solid gray) at various HPI (gray box value) is graphed. Note that all ordinal patterns have a non-zero frequency.

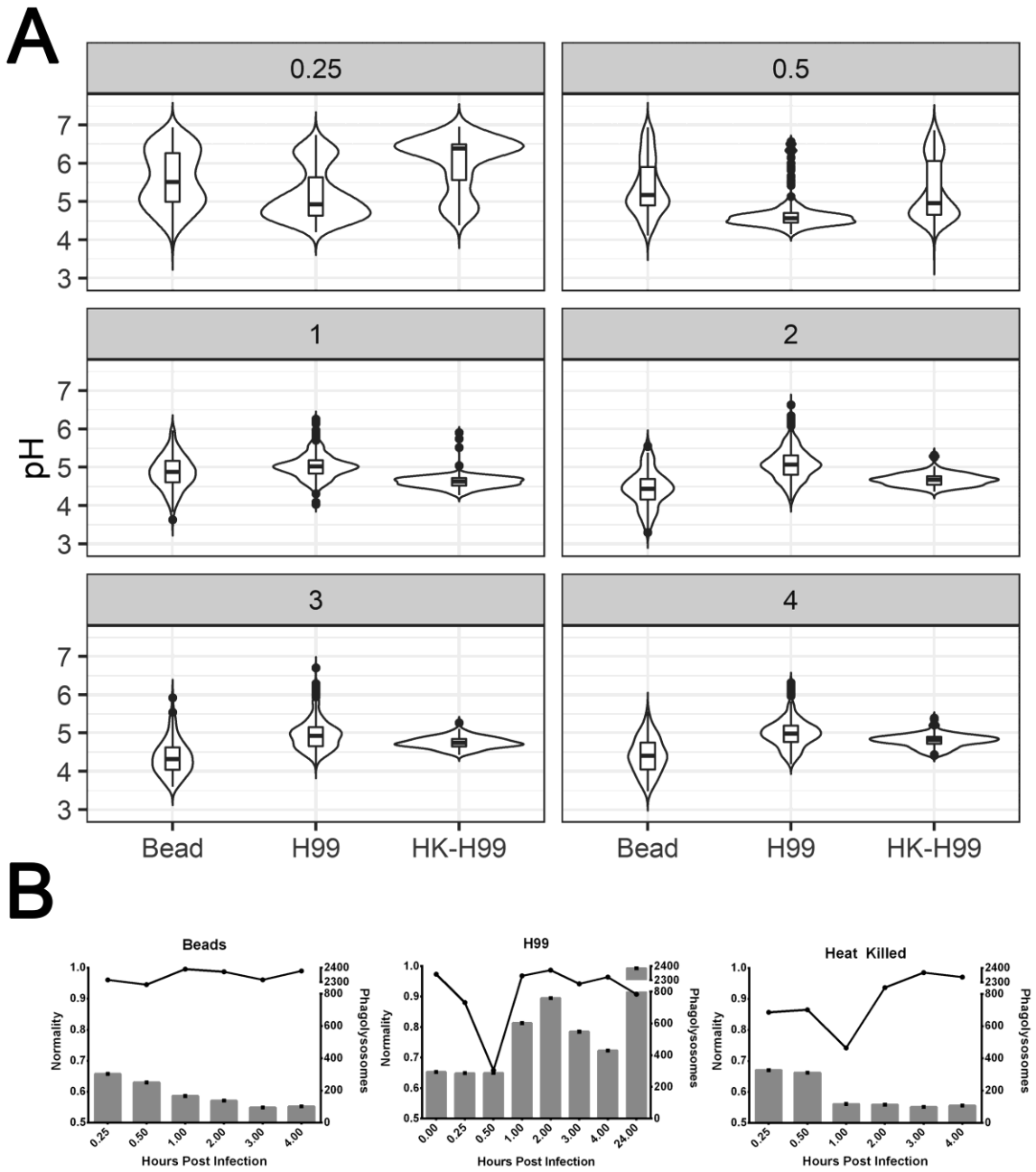

Figure 2. Bead ingested murine macrophage phagolysosomes stabilize to a normally distributed pH. **A.** Distributions of measured phagolysosomal pH after ingestion of various particles by BMDMs at various hours post infection (gray box value) for bead, live *C. neoformans* (H99), and dead *C. neoformans* (HK-H99). **B.** Visualization of estimated normality via Shapiro-Wilk (line) and total phagolysosome count (bar) for each sample.

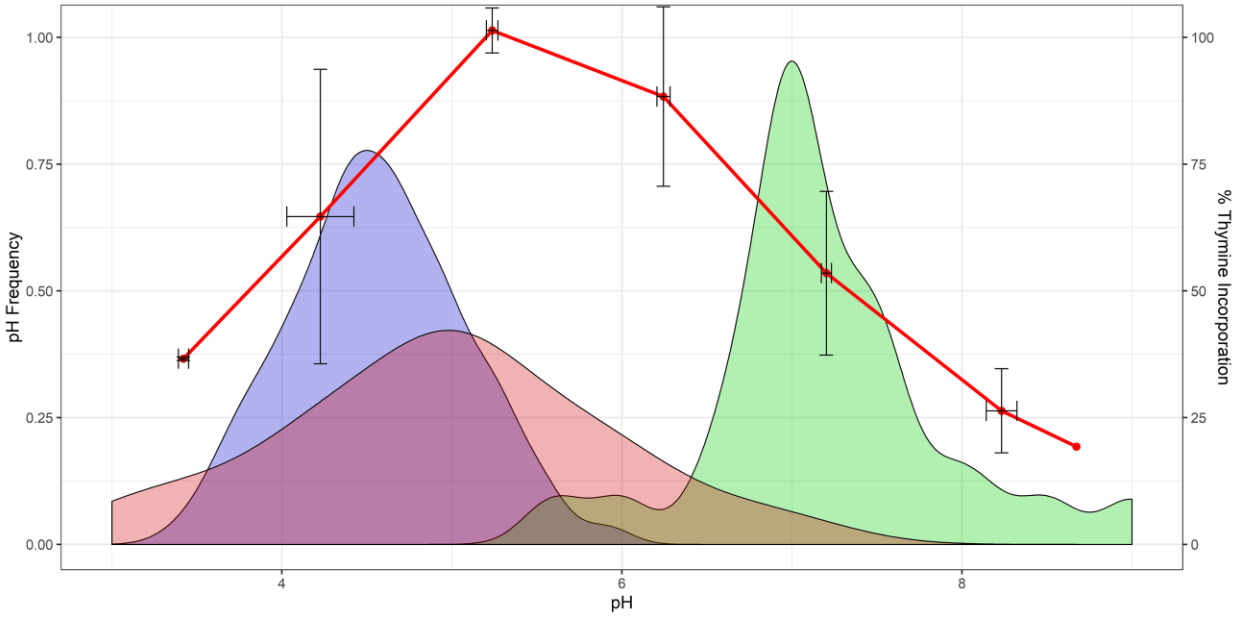

Figure 3. BMDM phagolysosomes acidify to a default pH range suboptimal for soil microbe and pathogen growth. Growth rates of soil bacteria(23, 24) as percent thymine incorporation (red line) and distribution of minimal culturable pH for 27 human pathogens (red fill) compared to the distribution of observed phagolysosomal pH after bead ingestion and phagolysosome maturation (blue fill). The bead pH distribution overlaps unfavorably with minimal growth conditions of microbes, and only minimally overlaps with the optimal growth pH range of the same 27 pathogens (green fill).

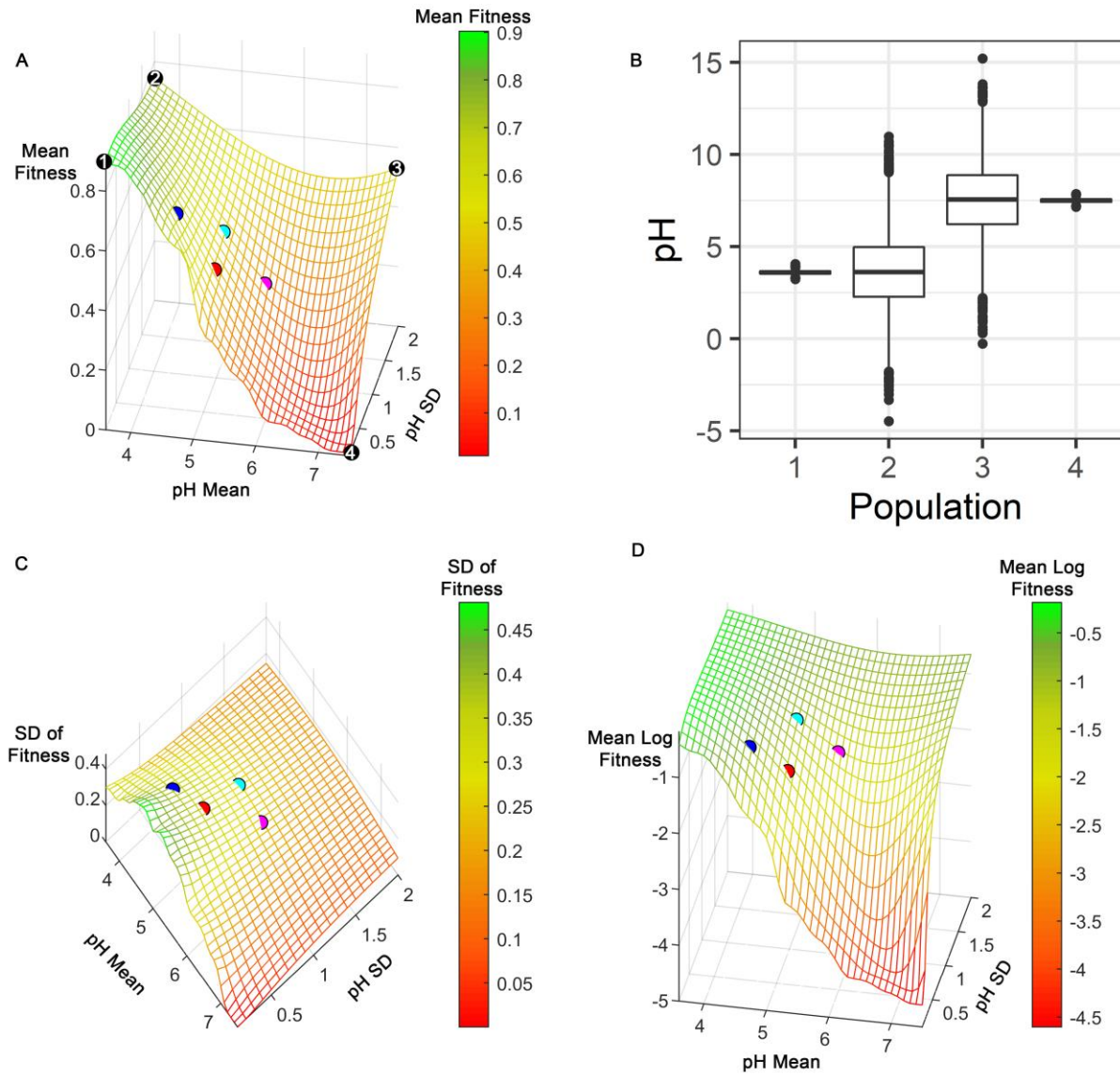

Figure 4. Simulated macrophage populations show stochastic pH as bet-hedging strategy. Success of host-microbe interactions are visualized as macrophage populations faced with randomly selected pathogens and acidified to random pHs from normal distributions of mean μ and standard deviation σ. Meshes represent host macrophage fitness, deviation in fitness, and log mean fitness. Plotted points represent measured data of H99 containing murine (red) and human (magenta) or bead containing murine (blue) and human (cyan) phagolysosomes. **A.** Mean macrophage survival (Z axis, colorbar) increases significantly as pH lowers, and mostly unchanged with standard deviation. **B.** Examples of simulated populations based on numbered points in panel A. Each combination of mean and SD from the axes of panel A represent a unique population of macrophages with a fitness represented by the Z axis and colored mesh. **C.** Deviation in host fitness (Z axis, colorbar) dramatically decreases by increasing standard deviation of pH, and mostly unaffected by shifts in mean pH. **D.** Logarithmic measurement of host fitness (Z axis, colorbar) to observe long term trends applicable to a bet-hedging strategy.

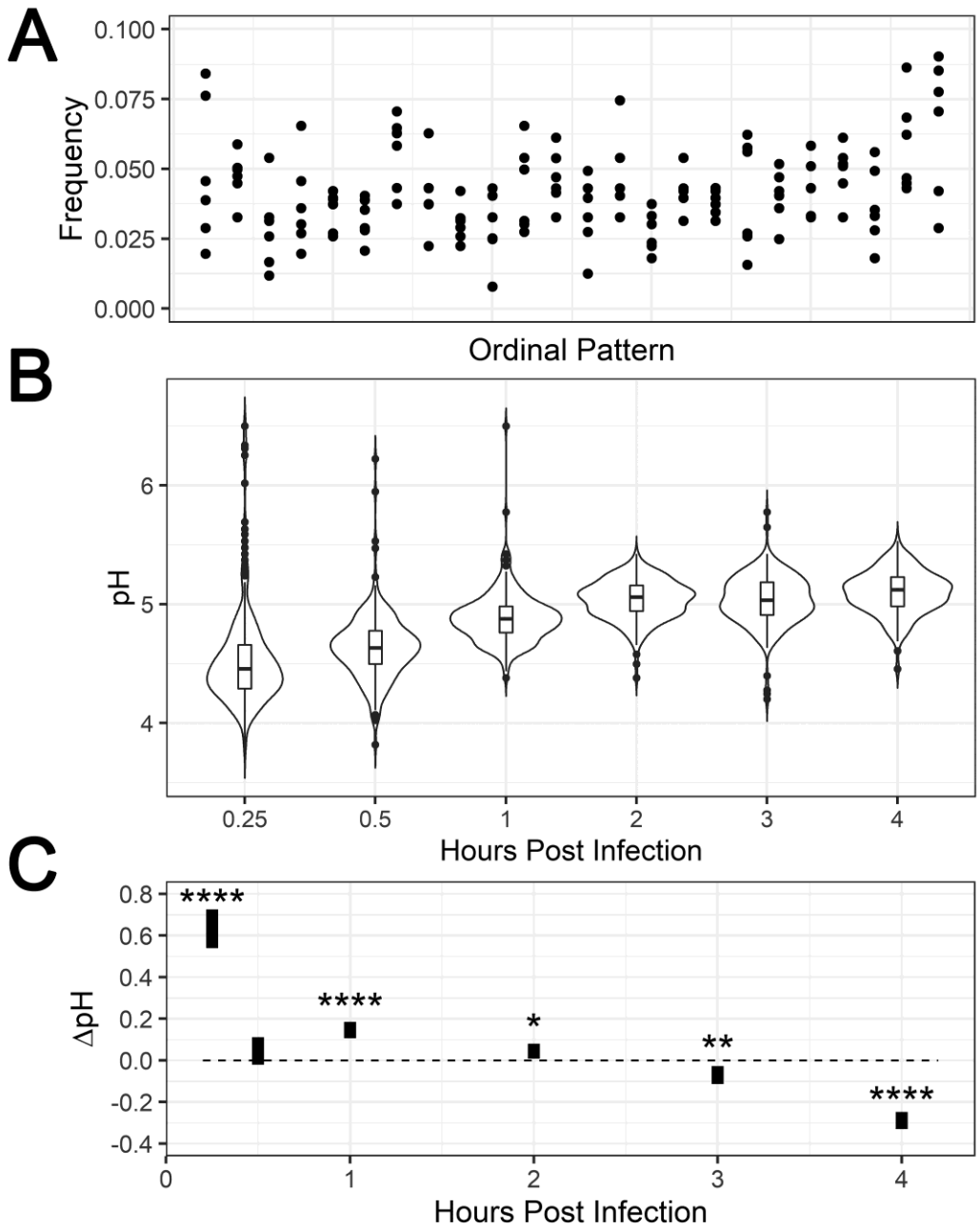

768

769 **Figure 5.** Trained murine macrophages have inverse acidification dynamics. **A.** Ordinal pattern analysis of
770 phagolysosome pH in trained BMDMs. All ordinal patterns appear at a non-zero frequency. **B.** pH
771 distributions of phagolysosomes at various HPI. **C.** Difference (95% CI) after subtracting mean trained
772 phagolysosome pH from mean untrained phagolysosome pH at each timepoint. *, **, **** denote $P <$
773 0.05, 0.01, and 0.0001 respectively via two tailed t-test.

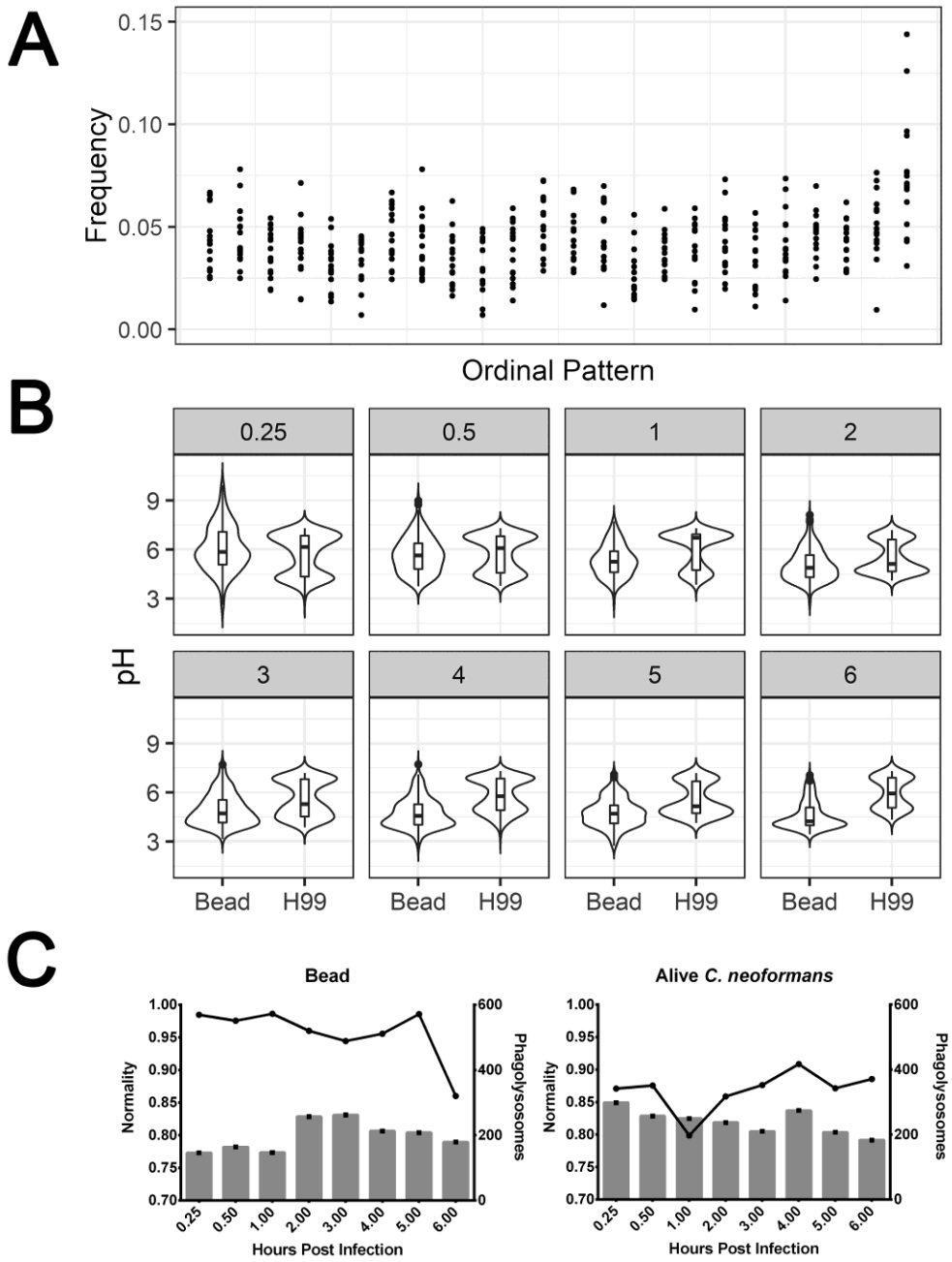

Figure 6. Isolated human monocytes acidify stochastically and approximate normality. Human macrophages were infected with inert beads or live *C. neoformans*, and their pH analyzed at various timepoints. **A.** Ordinal Pattern analysis for all conditions. All patterns exist at non-zero frequencies for all timepoints. **B.** Distributions of phagolysosome pH at different timepoints. **C.** Shapiro-Wilk normality and total sample count for each condition.

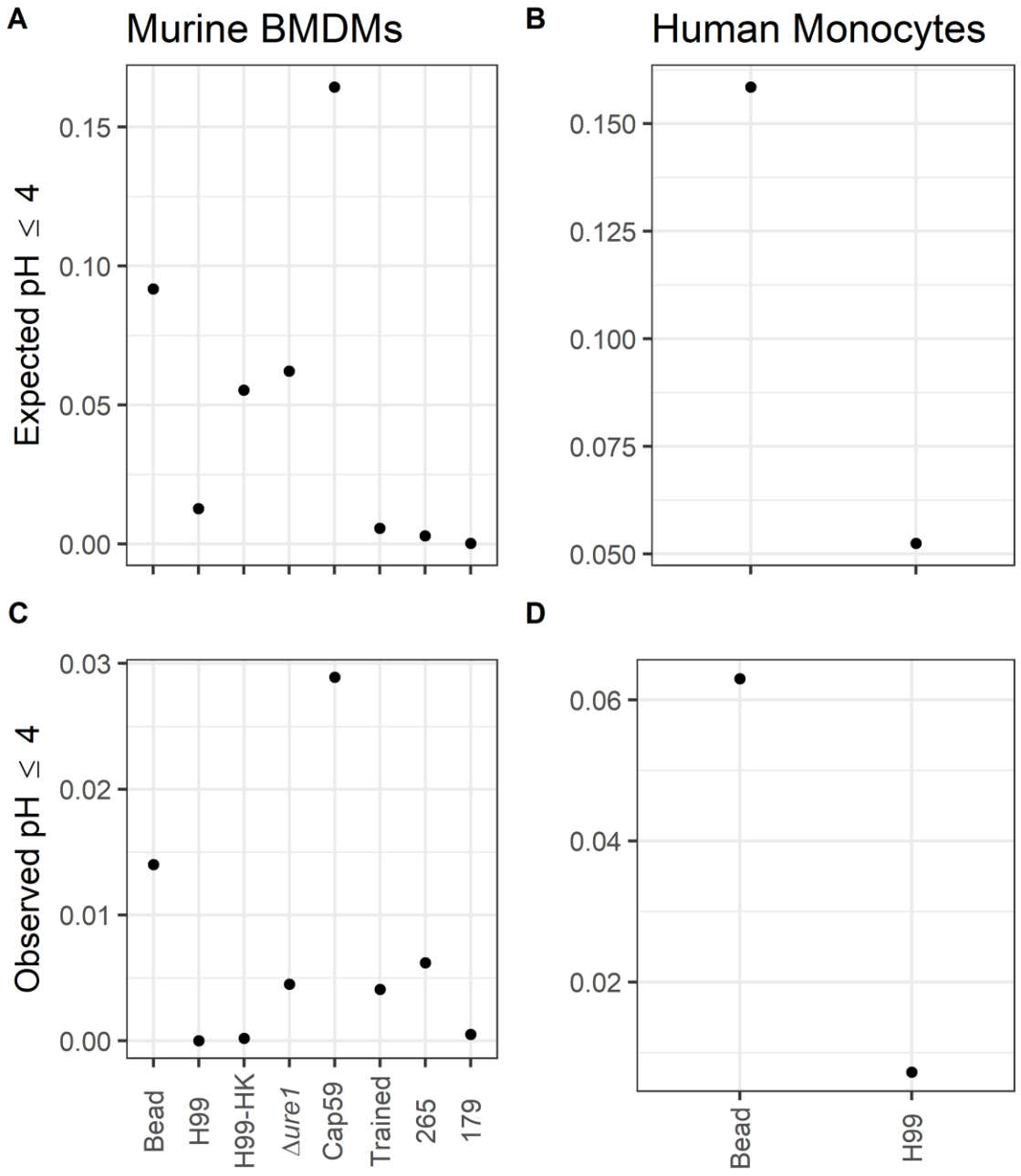

780

781 **Figure 7.** Expected and observed likelihood of phagolysosomes to achieve pH ≤ 4. **A.** The expected
782 proportions of murine BMDM phagolysosomes to achieve pH ≤ 4 assuming a normal distribution based
783 on the observed data. **B.** The expected proportions of human macrophage phagolysosomes to achieve pH
784 ≤ 4 assuming a normal distribution based on the observed data. Expected proportions of macrophages to
785 achieve pH ≤ 4 were calculated from a cumulative distribution function for a normal distribution whose
786 mean and standard deviation were calculated from the observed data. **C.** The observed proportions of
787 murine BMDM phagolysosomes to achieve pH ≤ 4. **D.** The observed proportions of human macrophage
788 phagolysosomes to achieve pH ≤ 4.

789

790 **Supplemental Information**

791 Supplemental Table-I: pH Susceptibility of Common Pathogens.

Microorganism	Inhibitory pH	Optimal Growth pH (range, average)	Reference
Acetinobacter baumannii	5	7	(52)
Bacillus cereus	4.3	6.75	(53)
Bartonella henselae	<6.6	6.8-7.2 (7.0)	(54)
Bacteroides fragilis	5	7-7.5 (7.25)	(55)
Bordetella pertusis	6	7-7.5 (7.25)	(56)
Brucella spp.	3.5	6.6-7.4 (7.0)	(57)
E. coli	~4	6-8 (7.0)	(58)
Campylobacter jujeni	4	6.5-7.5 (7.0)	(59)
Enterococcus spp.	4.5	7.5	(60)
Group A Streptococcus	5.5	7.5	(61, 62)
Group B Streptococcus	4.3	7	(63)
Histoplasma capsulatum	5	6-9 (7)	(64)
Legionella pneumophila	5	5.5-9.2 (7.35)	(65)
Listeria monocytogenes	3.3	5.6	(66, 67)
Mycobacterium tuberculosis	6.0	7.0	(68)
Mycobacterium avium	4.6	6	(69, 70)
Neisseria gonorrhea	5.8	6.7	(71, 72)
Neisseria menigitidis	6	7.2-9.0 (8.1)	(73)

Pseudomonas aeruginosa	5.4	6-7.5 (6.75)	(74)
Salmonella typhimurium	5	7	(75)
Staphylococcus aureus	4.3	6.5	(76)
Streptococcus pneumoniae	7.0	7.9	(77)
Serratia marcesens	3.0	9.0	(78, 79)
Shigella flexneri	5.5	7.5	(80)
Vibrio cholerae	5.0	8.5	(81, 82)
Yersinia enterocolitica	5.0		(83)
Yersinia pestis	5	7.6	(84, 85)

792 **Supplemental Table-I.** pH Susceptibility of Common Pathogens. pH tolerances of pathogens were found
793 through literature search. In the case of a range of optimal pH, the average was used for simulation data.
794 Species names are italicized.

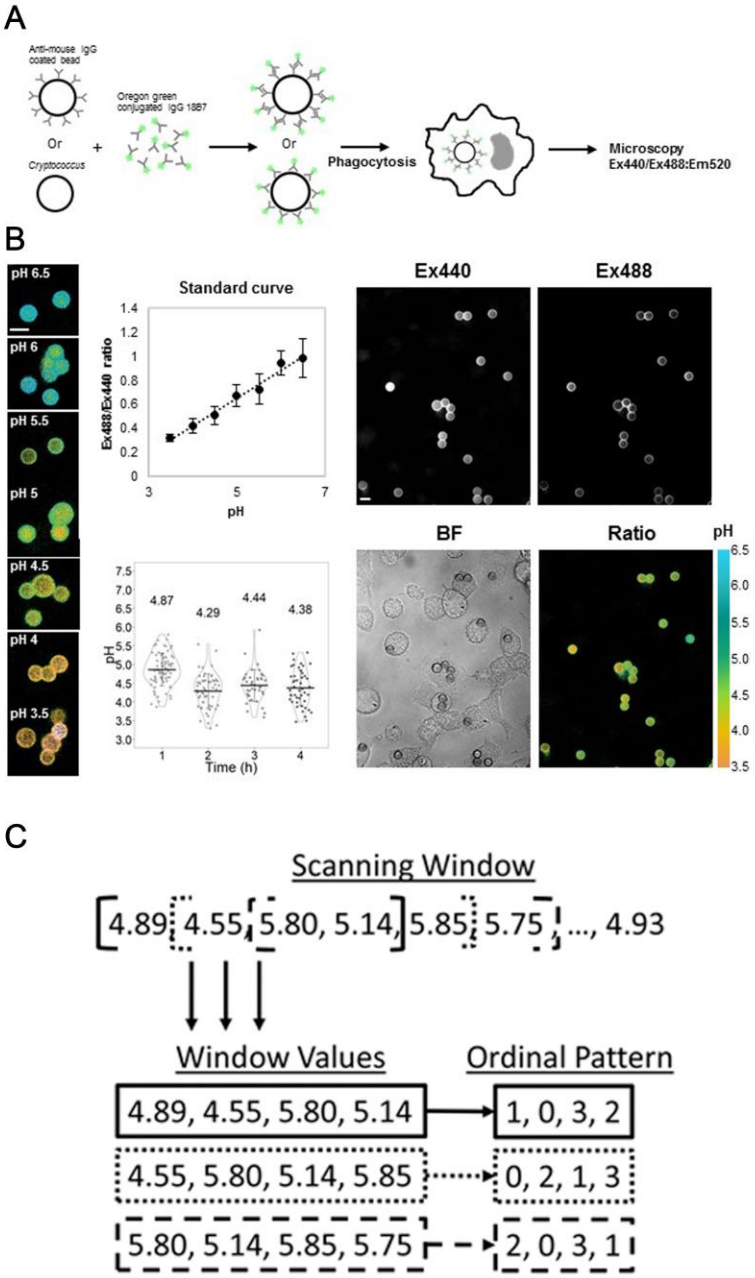

Supplemental Figure 1. Experimental designs for described methods. **A.** Experimental design for phagolysosomal pH measurement. Measurements are based on ratiometric measuring of Ex440/Em520 and Ex488/Em520. **B.** Experimental design for the detection of Chaos within a system. A scanning window generates sets of windows values which are analyzed for ordinal patterns.

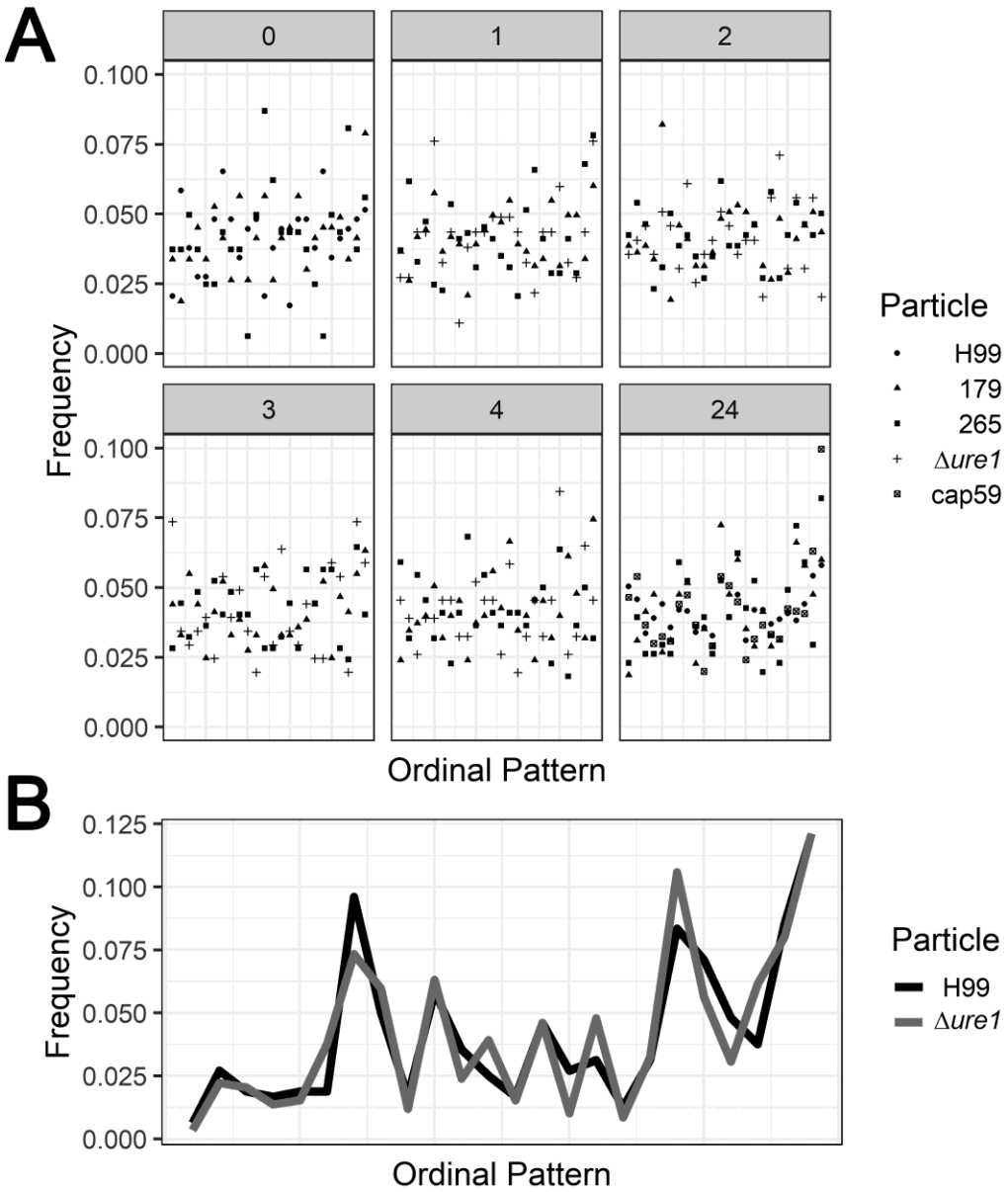

Supplemental Figure 2. Ordinal pattern analysis for expanded samples. **A.** Ordinal pattern frequencies for phagolysosomal acidification intervals in BMDMs infected with various particles at various hours post infection (gray box values). **B.** Ordinal pattern frequencies for time elapsed before initiation of budding for yeast strains ingested by BMDMs.

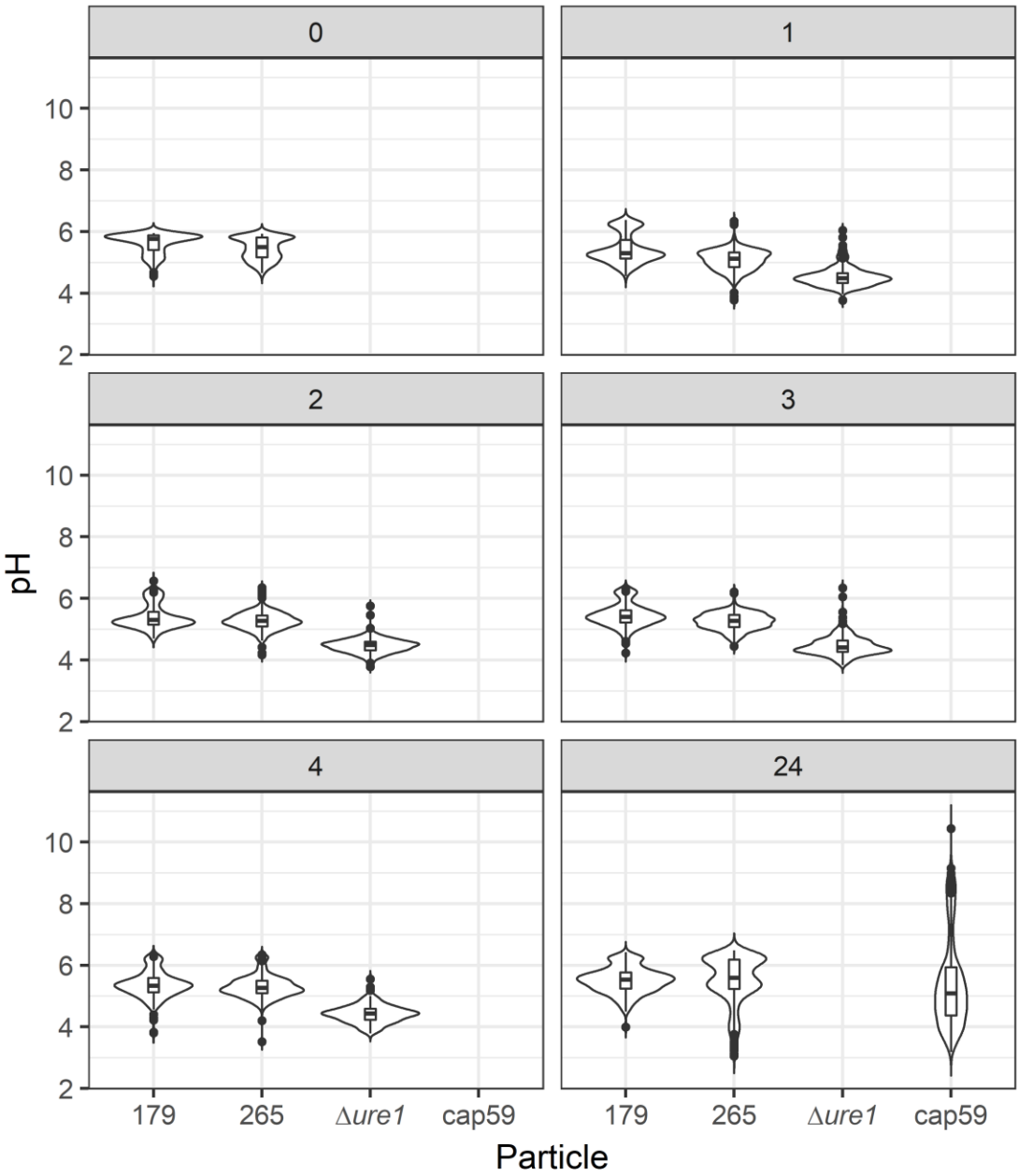

Supplemental Figure 3. Phagolysosomal pH distributions for expanded samples. Two strains of *C. gattii* (179 and 265), a urease deficient H99 mutant (*Δure1),* and a capsule deficient H99 mutant (cap59) were analyzed at various hours post infection (gray box value).

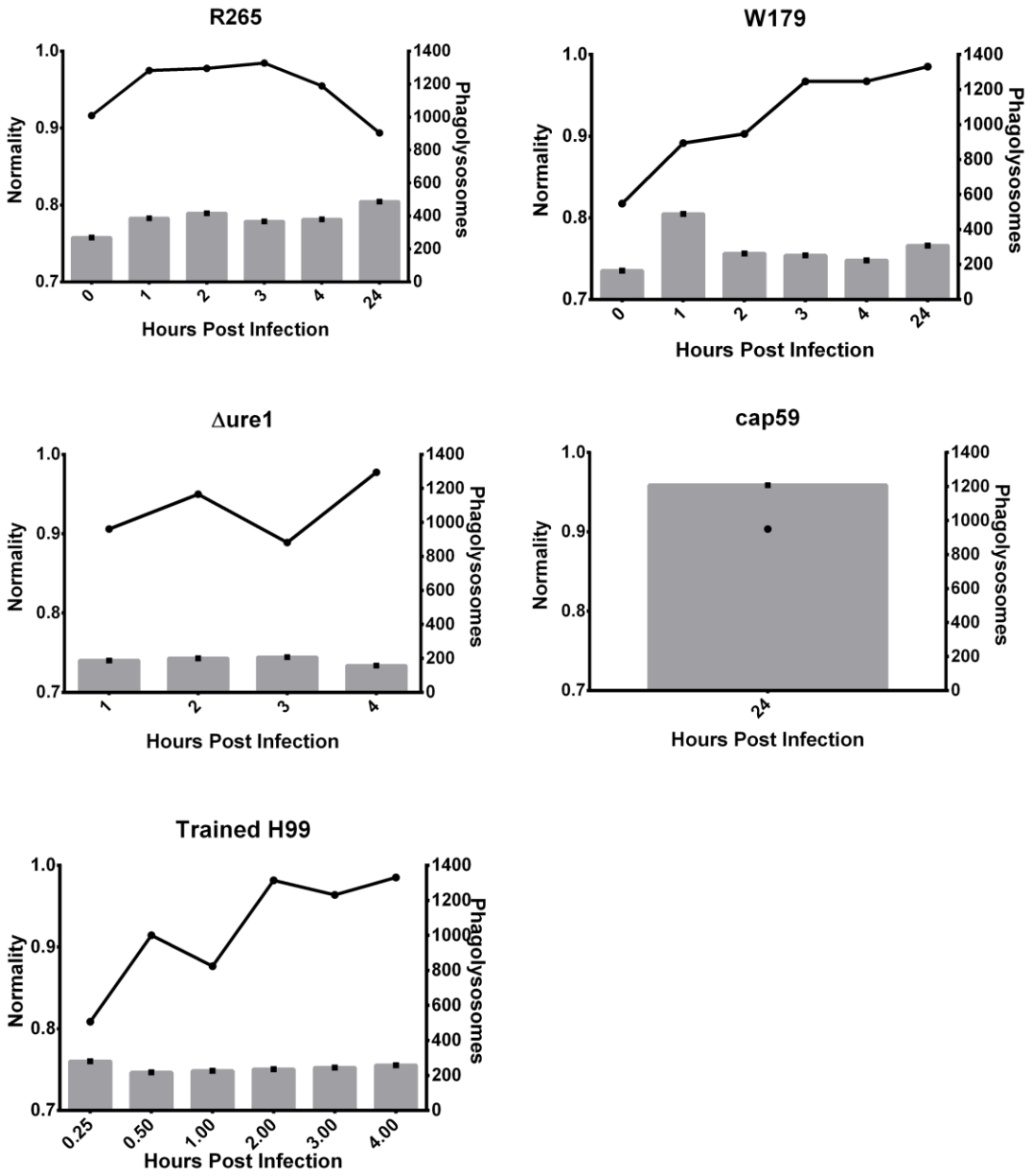

809

810 **Supplemental Figure 4.** Normality analysis for expanded samples. Shapiro-Wilk normality values (lines)
811 alongside total phagolysosome sample sizes (bars) for two strains of *C. gattii* (179 and 265), a urease
812 deficient H99 mutant (*Δure1),* a capsule deficient H99 mutant (cap59), and trained BMDMs on reinfection.

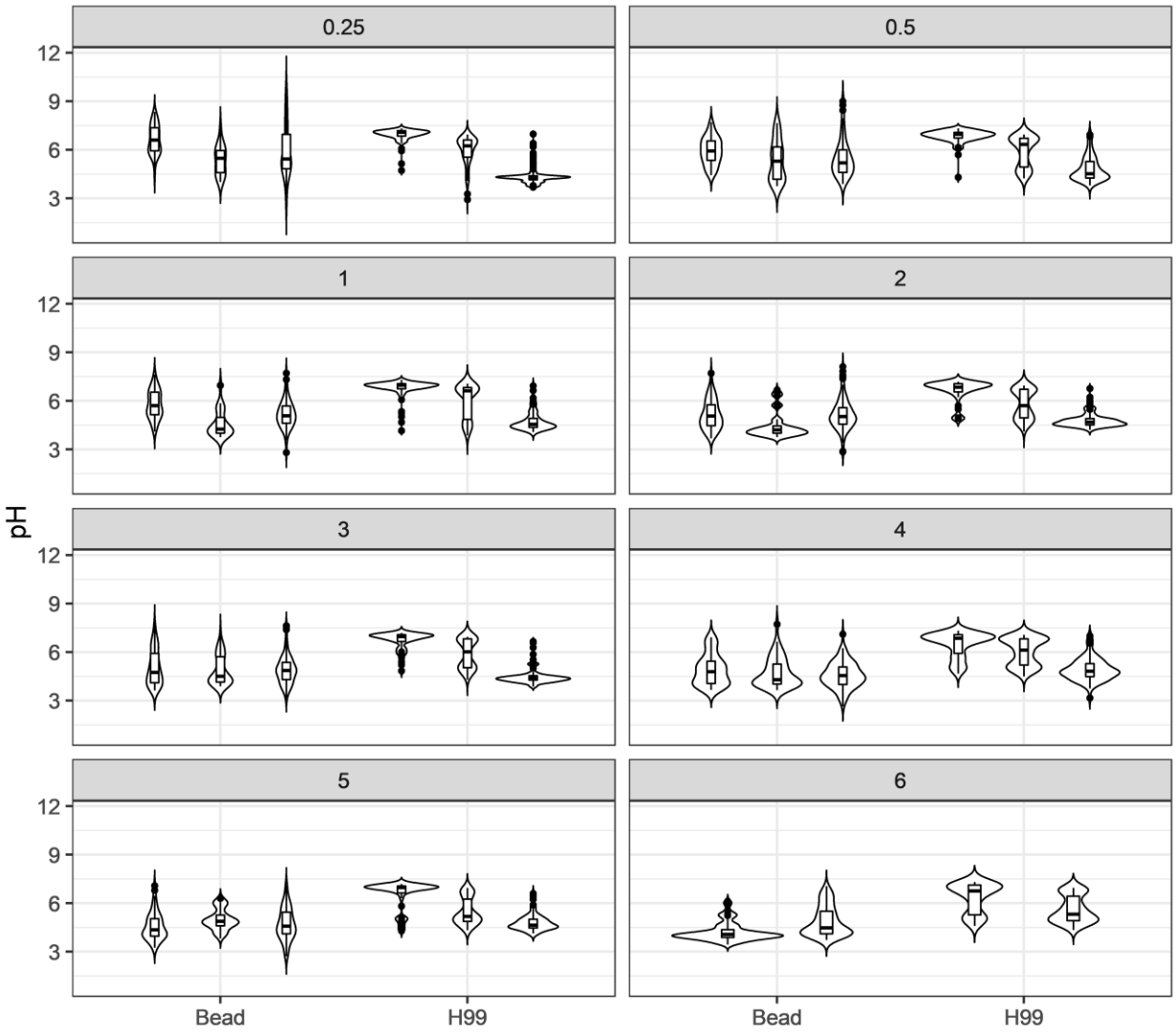

813

814 **Supplemental Figure 5.** Phagolysosomal pH distributions for human macrophages infected with H99
815 separated by individual donor. Human macrophages were analyzed after ingesting either H99 or inert
816 beads at various hours post infection (gray box value).